PARAMETERIZATION OF THE SOLAR ABSORPTIVITY AND TRANSMISSIVITY USING NIMBUS II REFLECTANCE DATA

Donald Jeremiah Healy

NAVAL POSTGRADUATE SCHOOL
Monterey, California

THESIS

PARAMETERIZATION OF THE
SOLAR ABSORPTIVITY AND TRANSMISSIVITY
USING NIMBUS II REFLECTANCE DATA

by

Donald Jeremiah Healy

September 1974

Thesis Advisor: F. L. Martin

SECURITY CLASSIFICATION OF THIS PAGE (When Data Entered)

REPORT DOCUMENTATION PAGE

READ INSTRUCTIONS BEFORE COMPLETING FORM

1. REPORT NUMBER	2. GOVT ACCESSION NO. / 3. RECIPIENT'S CATALOG NUMBER
4. TITLE (and Subtitle): Parameterization of Solar Absorptivity and Transmissivity based On NIMBUS II	5. TYPE OF REPORT & PERIOD COVERED: Master's Thesis, September 1974
	6. PERFORMING ORG. REPORT NUMBER
7. AUTHOR(s): Donald Jeremiah Healy	8. CONTRACT OR GRANT NUMBER(s)
9. PERFORMING ORGANIZATION NAME AND ADDRESS: Naval Postgraduate School, Monterey, California 93940	10. PROGRAM ELEMENT, PROJECT, TASK AREA & WORK UNIT NUMBERS
11. CONTROLLING OFFICE NAME AND ADDRESS: Naval Postgraduate School, Monterey, California 93940	12. REPORT DATE: September 1974
	13. NUMBER OF PAGES
14. MONITORING AGENCY NAME & ADDRESS (if different from Controlling Office): Naval Postgraduate School, Monterey, California 93940	15. SECURITY CLASS. (of this report): Unclassified
	15a. DECLASSIFICATION/DOWNGRADING SCHEDULE

16. DISTRIBUTION STATEMENT (of this Report)

Approved for public release; distribution unlimited.

17. DISTRIBUTION STATEMENT (of the abstract entered in Block 20, if different from Report)

18. SUPPLEMENTARY NOTES

19. KEY WORDS (Continue on reverse side if necessary and identify by block number)

Solar Budget
Absorptivity
Transmissivity

20. ABSTRACT (Continue on reverse side if necessary and identify by block number)

Satellite data first became available in the 1960's making solar budget calculations more feasible. In this study, satellite measurements of reflected solar insolation from NIMBUS II were combined with simultaneous pyrheliometer readings of transmissivity over North America to provide the basis for computation of the atmospheric absorptivity. In the statistical parameterization of the absorptivity, such readily available data as water

DD FORM 1 JAN 73 1473 EDITION OF 1 NOV 65 IS OBSOLETE
S/N 0102-014-6601 |
(Page 1)

SECURITY CLASSIFICATION OF THIS PAGE (When Data Entered)

vapor mass and satellite reflectance were introduced as independent variables in the regression equations. Correlation coefficients between observed regression-determined absorptivities and transmissivities were computed based upon an initial total of 235 data-samples, and the results interpreted. The conclusion was twofold: (1) A new suggested insolation-budget model is proposed for computation of absorptivity;. (2) the desirability of deriving a statistical parameterization for cloud-cover at grid points in terms of satellite-observed reflectances and window-channel temperatures is shown.

Parameterization of the Solar Absorptivity and Transmissivity Using Nimbus II Reflectance Data

by

Donald Jeremiah Healy
Lieutenant, United States Navy
B.S., United States Naval Academy, 1968

Submitted in partial fulfillment of the requirements for the degree of

MASTER OF SCIENCE IN METEOROLOGY

from the

NAVAL POSTGRADUATE SCHOOL
September 1974

ABSTRACT

Satellite data first became available in the 1960's making solar budget calculations more feasible. In this study, satellite measurements of reflected solar insolation from NIMBUS II were combined with simultaneous pyrheliometer readings of transmissivity over North America to provide the basis for computation of the atmospheric absorptivity. In the statistical parameterization of the absorptivity, such readily available data as water vapor mass and satellite reflectance were introduced as independent variables in the regression equations. Correlation coefficients between observed regression-determined absorptivities and transmissivities were computed based upon an initial total of 235 data-samples, and the results interpreted. The conclusion was twofold: (1) A new suggested insolation-budget model is proposed for computation of absorptivity; (2) the desirability of deriving a statistical parameterization for cloud-cover at grid points in terms of satellite-observed reflectances and window-channel temperatures is shown.

TABLE OF CONTENTS

LIST OF TABLES

LIST OF FIGURES

Page

ACKNOWLEDGEMENTS

The author wishes to take this opportunity to express his appreciation to his advisor, Professor F. L. Martin, for his patient assistance and guidance in the research and preparation of this paper. Also to the W. R. Church Computer Facility of the Naval Postgraduate School for the use of the IBM 360 Computer.

A very warm thanks to my wife for her typing assistance and encouragement in the preparation of this paper.

I. INTRODUCTION

The solar energy cycle is of vast importance to the meteorological community since addition of heat is a primary source of energy in atmospheric circulations. Therefore, a proper accounting of absorptivity and transmissivity within the atmosphere is vital to improved modeling and numerical forecast procedures.

This study is designed to correlate satellite measurements of reflected solar insolation from the Medium Resolution Infrared Radiometer (MRIR) on NIMBUS II and simultaneous pyrheliometer readings of transmissivity over North America. This research was directed towards the parameterization of the atmospheric absorptivity and transmissivity in terms of available satellite albedo observations. In addition such other readily available data such as water vapor mass and cloud-cover may be introduced for perfecting the parameterization.

The limits of the study were confined to the United States and Canada where data were readily available.

Studies of the disposition of solar insolation prior to the acquisition of satellite data have been reported by Gabites (1950), London (1957) and Sellers (1965). Each of these researchers gave estimates of global albedo of close to 35%. Vonder Haar (1968) using satellite data, has shown the global albedo to be close to 30%. In view of this

reduction of the albedo of 5% from the previous estimates, one should look for revised transmissivity and absorptivity parameterizations which would account for the insolation balance.

It would seem that successful parameterization of absorptivity and transmissivity could be accomplished over data-rich areas such as existed over North America during the NIMBUS II period of this study. In the long-term, one would hope to describe these variables of the solar budget in terms of readily accessible satellite observations, and ultimately expand the parameterization to oceanic and other data-sparse areas.

II. DATA SOURCES AND PROBLEM OUTLINE

A. GENERAL

The data used in this study was from three basic sources and covered a five-day period from 15 July 1966 to 20 July 1966. The surface data were compiled at the 47 pyrheliometric stations shown in Fig. 1. The locations were chosen to provide a broad coverage of solar transmission effects on the North American continent within the limits 25° north latitude to 59° north latitude. Several other types of data compilations (described below) were required to perform computations of solar reflectance, transmittance, and absorptivity at pyrheliometric stations at the effective time of the NIMBUS II scan time. Thus all observational data had to be interpolated to local solar times corresponding to the effective scan time of the NIMBUS II satellite at the pyrheliometric station. Solar time is computed everywhere on the basis that 1200 solar time corresponds to the highest solar elevation of the day.

B. NIMBUS II REFLECTANCE DATA

NIMBUS II solar reflectance values were available for this study only in hard copy printout format. The NIMBUS II satellite had a nearly sun-synchronous polar orbit with the ascending node at 11:28 (equatorial solar time). The satellite scanned a swath perpendicular (Fig. 2) to its

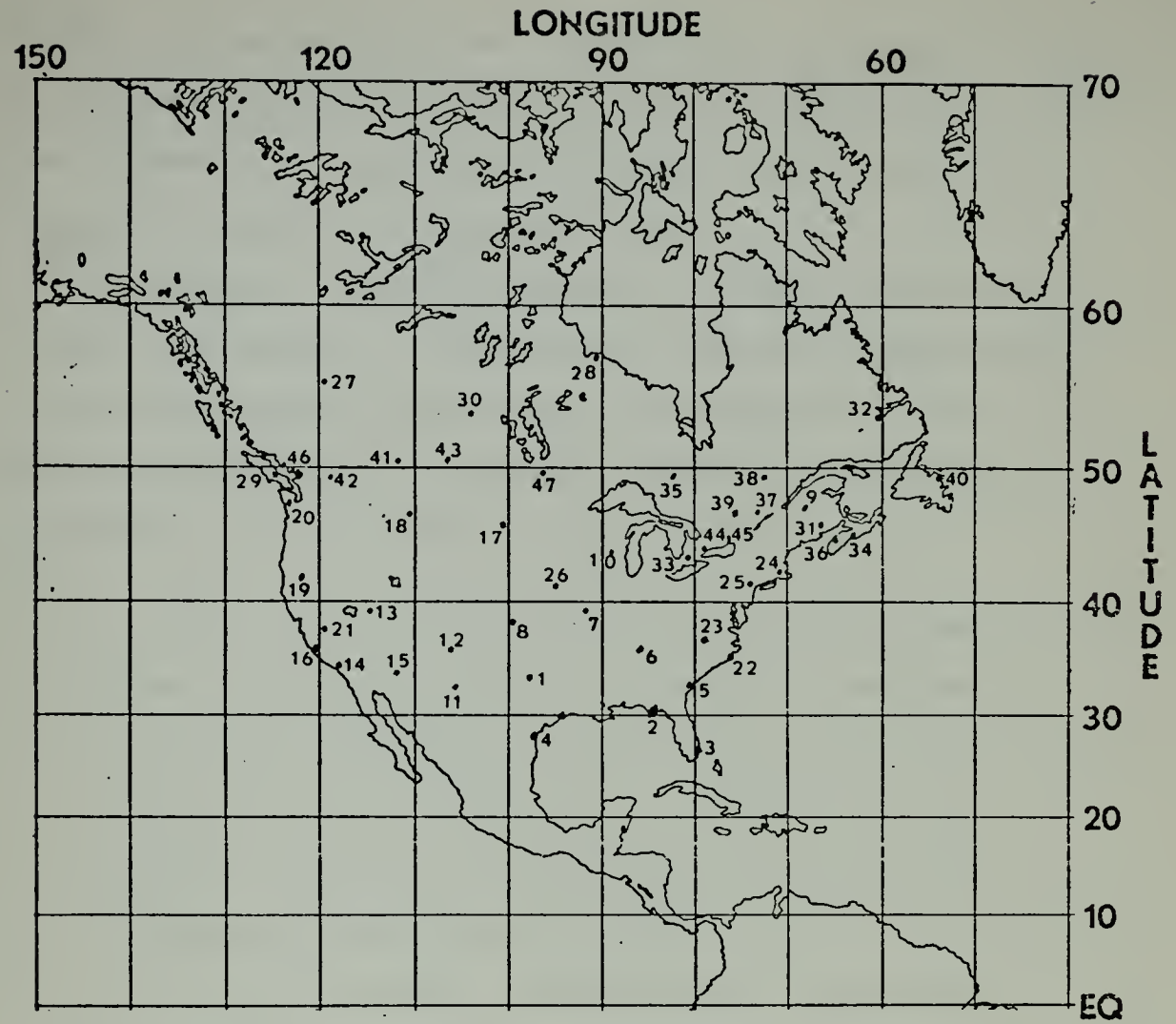

Figure 1 - Mercator map-projection of data region showing pyrheliometer station locations used in this study. Detailed latitude and longitude values for each station are located in Appendix Table A.

orbit, and extending between the horizons. Each scan spot is approximately a 30-mile square at the subsatellite point and increases in size with increasing nadir angle of the scan spot relative to the satellite.

The NIMBUS II Medium Resolution Infrared Radiometer (MRIR) was designed to scan in the five wavelength regions (listed below) with each region accompanied here by a brief description of the observational purpose of channel observation (e.g., NIMBUS II User's Guide, 1966).

6.4 to 6.9 microns - This channel covers the 6.7 micron water vapor absorption band. Its purpose is to provide information on water vapor distribution in the upper troposphere and, in conjunction with the other channels to provide data concerning relative humidities at these altitudes.

10 to 11 microns - Operating in an atmospheric "window," this channel measures surface or near-surface temperatures over clear portions of the atmosphere. It also provides cloud cover and cloud height information (day and night).

14 to 16 microns - This channel, centered about the strong absorption band of CO_2 at 15 microns, measures radiation which emanates primarily from the stratosphere. The information gained here is of primary importance in following the seasonal stratospheric temperature changes.

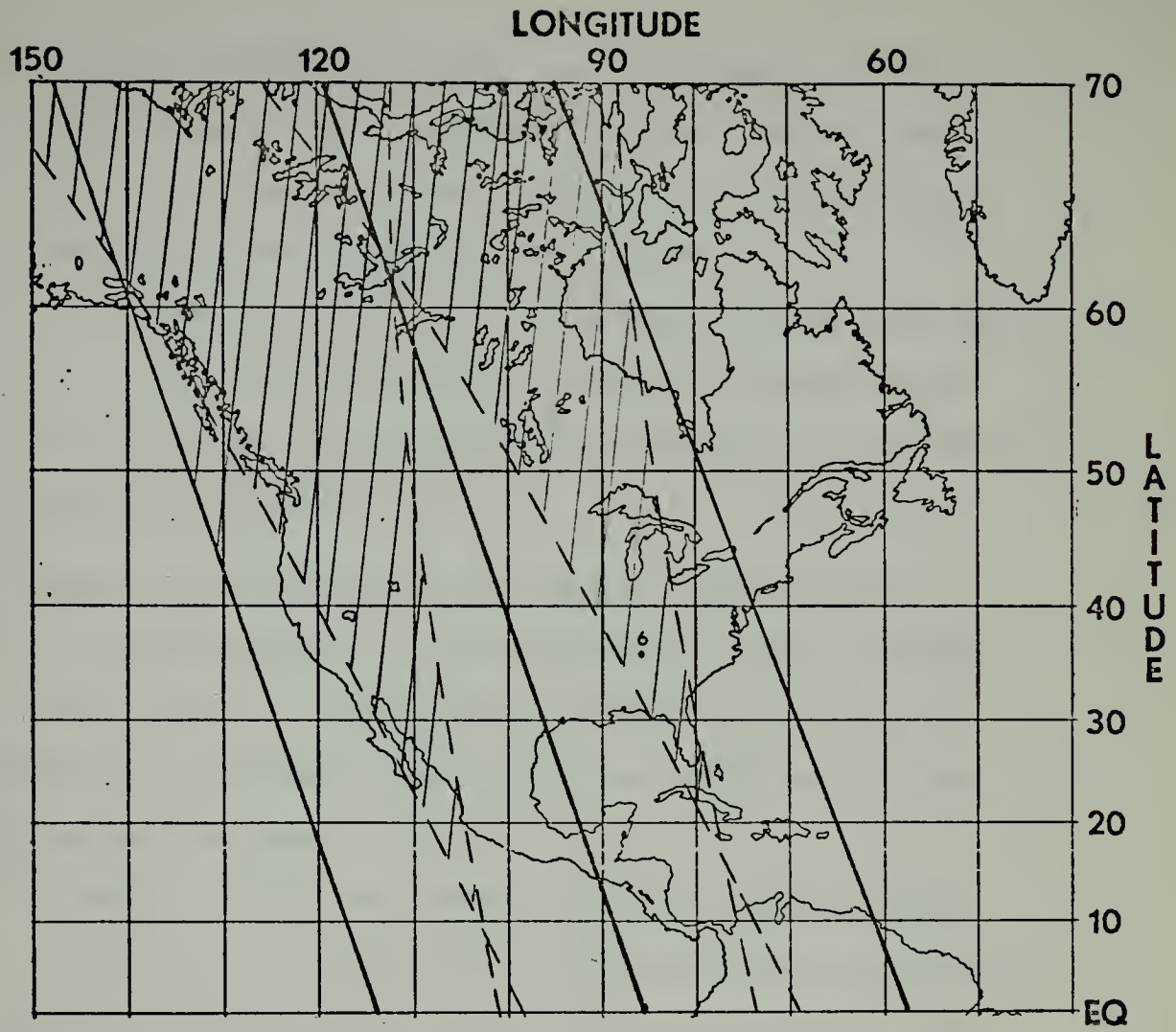

Figure 2 - Mercator map showing NIMBUS II orbital paths as indicated by the solid lines —. The limits of the swath coverage are indicated by the dashed lines --. Overlapped regions are indicated by the cross hatching//.

5 to 30 microns - This channel measures the emitted long wavelength infrared flux and, in conjunction with the reflected solar radiation channel furnishes data on the heat budget of the planet.

0.2 to 4.0 microns - This channel covers more than 99% of the solar spectrum and yields information on the intensity of reflected solar energy from the earth and its atmosphere.

These five channels are frequently termed channels 1, 2, ..., 5, respectively, of the MRIR experiment of NIMBUS II. Of the various channel-data available, only channel 5 relating to solar reflectance from the earth and its atmosphere was utilized.

It would perhaps have been a useful indirect measure of cloud cover to have used the "window" channel-equivalent blackbody temperature data for the same observation times. However, synoptic surface temperatures at the pyrheliometric stations would have been necessary to give a concise indication of the cloud amount and/or height, so that the channel 2 data were not analyzed here.

The effective radiant reflectance R in the direction of the satellite from the reflecting surface filling the field of view of the radiometer and illuminated by unattenuated solar radiation is defined (p. 57, NIMBUS II Users' Guide, 1966) by

$$R(I',J',Z') = \frac{N(I',J',Z')}{\frac{Sr_m^2}{r^2}\cos Z'} \qquad (1)$$

where I',J' are the coordinates of the scan spot, Z' is the zenith angle of the sun and

$$H = \frac{Sr_m^2}{r^2} \qquad (2)$$

is the date-adjusted value of the solar constant S (corrected to 17 July 1966). The parameter N in (1) is the solar intensity or radiance in watts m^{-2} $ster^{-1}$ reflected back to the satellite, and is here assumed independent of the viewing angles (nadir and azimuth) of the satellite relative to the scan spot. The latter assumption is not actually valid as has been shown by Raschke et al. (1973) who showed the distribution of the bidirectional reflectance over typical land spots to be dependent upon both angles. However, our scan-spot reflectances were computed by NASA according to Eq. 1. The hard-copy reflectance data obtained from NASA were in the form of averages composited to gridpoints on a Mercator map projection of scale 1:10M (Fig. 3) and with a grid-mesh (I,J). This (I,J) grid-mesh may be formulated in terms of longitude λ and latitude Φ by means of the transformation:

$$I - 1 = 0.8(150^\circ - \lambda^\circ) \qquad (3)$$

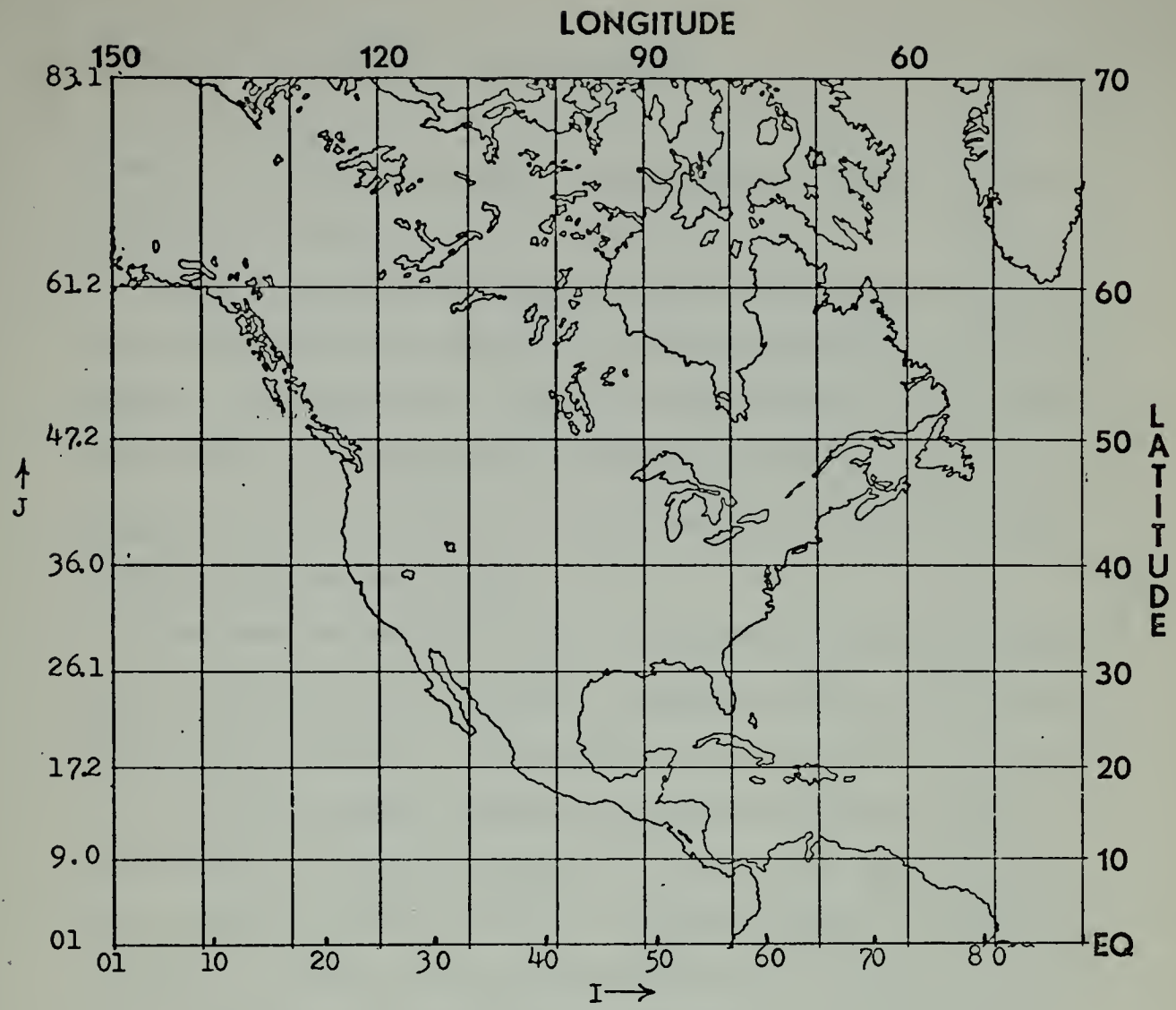

Figure 3 - Mercator map-projection of data region used in analysis of data considered in this study. Equally spaced I- and J- intervals are indicated along the bottom and left boundaries of the rectangular area. Corresponding longitude and latitudes are shown along the opposite boundaries.

$$J - 1 = 0.8\left(\frac{180}{\pi}\right) \ln \left(\frac{1 + \sin \phi}{\cos \phi}\right) \qquad (4)$$

Some of the NIMBUS II data orbits used on 16 July 1966 are sketched in Fig. 2.

Within any grid space centered at (I,J) the number of scan spots may vary from five to ten depending on the nadir angle to the scan spot, the actual earth-size of the grid-area (which is determined by the map factor $m = \sec \phi$, $d_E = d_{map}/m$), and the extent of swath overlap at the scan spot between successive orbits.

The mean reflectance value obtained at each grid point (I,J) is therefore an average composited from all of the individual scan-spot reflectances R(I,J,I',J',Z'). Here I',J' are individual scan spots contained in the larger grid-mesh I,J of the map (Fig. 3) within the grid square. The averaged value $R(I,J,\bar{Z})$ is the mean solar reflectance to space, computed after averaging over all the scan spots I',J' within I,J and is a function only of the gridpoint identifiers (I,J) and of $\bar{Z}$, the mean solar zenith angle at (I,J). $R(I,J,\bar{Z})$ as thus determined is termed the directional reflectance at the grid point, the direction being that of the mean solar zenith angle to the center of the grid square. Thus after the averaging reflectances to grid points has been accomplished, the resulting reflectance $R(I,J,\bar{Z})$ is given by:

$$R(I,J,\bar{Z}) = \pi \bar{N} \Big/ \left[S\left(\frac{r_m}{r}\right)^2 \cos \bar{Z} \right] \qquad (5)$$

where

S = solar constant = 2.0 langleys min^{-1}

$\cos \bar{Z}$ = mean cosine of the solar zenity angle subtended by point I,J at station.

$$\cos \bar{Z} = \cos \phi \cos \delta \cos h + \sin \phi \sin \delta \qquad (6)$$

ϕ = station latitude

δ = solar declination

h = hour angle at effective time of satellite scan.

$\bar{N}$ = mean reflected solar radiance from (I,J) to the satellite.

(r_m/r) = ratio of the mean distance to the sun and the distance to the sun at the required time.

1. Effective Time Calculation

The effective Greenwich Mean Time of the satellite reflectance observation at any station was computed using a linear interpolation scheme between the times along the swath over the station and orthogonal to successive satellite tracks, and the stations distances relative to the tracks as shown by Fig. 4. Thus Eq. (7) is used to interpolate for effective time over the station as shown in Fig. 4.

$$\text{Effective scan-time} = \left(\frac{\Delta X}{X}\right)(T_2) + \left(\frac{X-\Delta X}{X}\right)(T_1) \qquad (7)$$

If the station was in a region scanned only by one swath, the time T_1 was read directly off the nearest track in

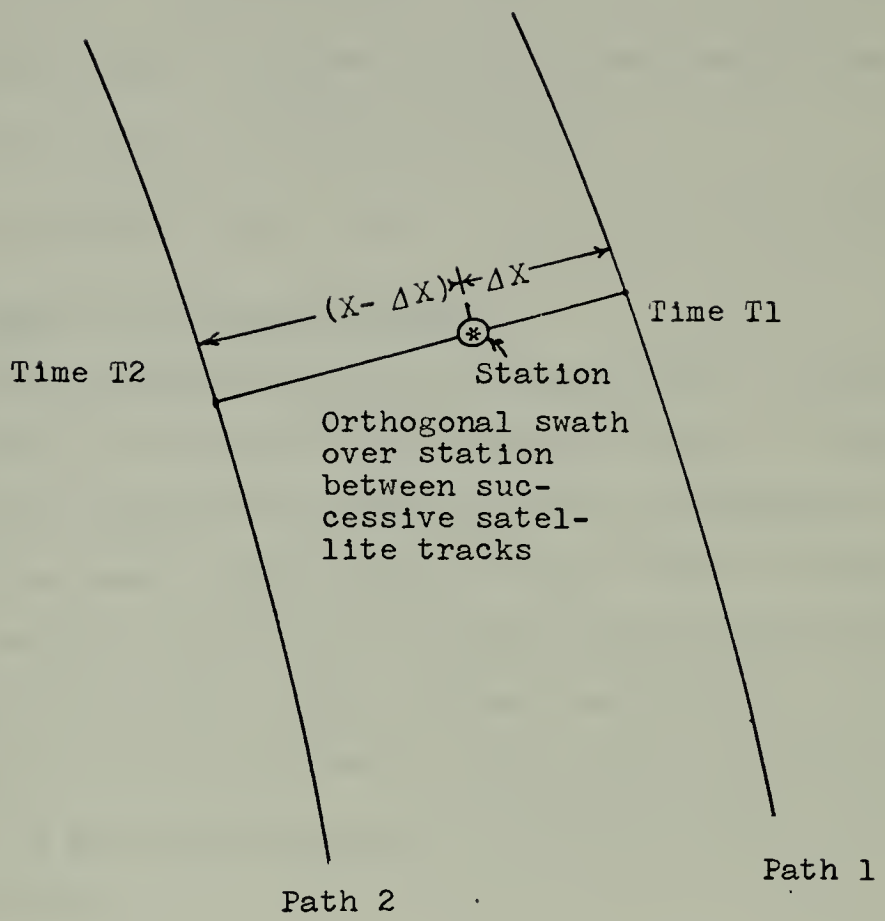

Figure 4. Interpolated Scan-Time

Fig. 2. The effective time T was then converted to true solar time for the station by the following equation:

$$S.T. = T(GMT) - \frac{(LONG.DEG)}{15(LONG.DEG)} * (HRS) \qquad (8)$$

Note the hour angle h depends upon the solar time of the scan as given by Eq. 9 and has the form:

$$h = S.T.(hours) - 12 * 15^{o} \qquad (9)$$

2. Station Reflectance Values

The pyrheliometer station location (Fig. 1) falls within groups of four grid points shown in Fig. 5. Therefore, a linear interpolation scheme was used to determine a value for the exact station location (I+ΔI, J+ΔJ) located between the four adjacent grid points at which the reflectance values R(A), R(B), R(C), R(D) were available. The reflectance value at the location I+ΔI, J+ΔJ (the station location) is given by means of the standard spatial interpolation formula .

$$R = (1-\Delta J)\left[(1-\Delta I)R(A)+\Delta I*R(B)\right] +\Delta J\left[(1-\Delta I)R(D) +\Delta I*R(C)\right] \qquad (10)$$

Here R(A) is the reflectance at point A, R(B) is that at B, etc., as indicated by the grid array in Fig. 5.

C. SURFACE TRANSMITTANCE OF SOLAR INSOLATION

Surface transmittance of solar radiation was based on pyrheliometer readings recorded at the stations in Fig. 1.

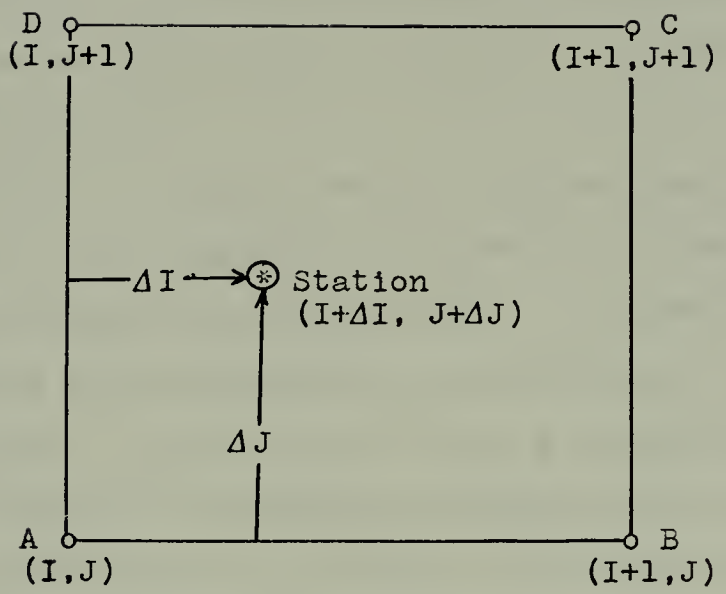

Figure 5. Reflectance-Interpolation to Stations.

These records provided on magnetic tape are listings of the hourly accumulations of solar insolation observed at the end of each true solar hour. The taped record was kindly furnished with the technical assistance of the Commander, Naval Weather Service. The values listed were pyrheliometer readings of the total hemispheric insolation, with the pyrheliometer calibrated to conform to a solar constant of 2.0 langleys min^{-1}.

The locations of pyrheliometric stations were converted from latitude ϕ and longitude λ to the (I,J) coordinate system in accordance with Eqs. 3 and 4. The mean station transmittances were determined at the effective time of the satellite scan. This was done to give a transmittance coincident with the "simultaneous" satellite mean reflectance observations over this station. The actual station insolation was considered to be time-centered at 0930 solar hours when it was reported for the solar hour ending at 1000, etc. Thus, it was necessary to interpolate an insolation value at the station coincident with the effective time of the satellite-scan. This was accomplished by using a cubic Lagrangian time-interpolation scheme described below.

The four successive values of the hourly insolation that bracketed the effective scan time were used in the following equation:

$$Q_G = \frac{(T-T2)*(T-T3)*(T-T4)*Q1}{(T1-T2)*(T1-T3)*(T1-T4)} + \frac{(T-T1)*(T-T3)*(T-T4)*Q2}{(T2-T1)*(T2-T3)*(T2-T4)}$$

$$+ \frac{(T-T1)*(T-T2)*(T-T4)*Q3}{(T3-T1)*(T3-T2)*(T3-T4)} + \frac{(T-T1)*(T-T2)*(T-T3)*Q4}{(T4-T1)*(T4-T2)*(T4-T3)} \quad (11)$$

Here

Q_G = station insolation interpolated to the scan time.

T = effective time of satellite-scan.

T1,T2,T3,T4 = successive times of pyrheliometric readings at half-hour solar clock times.

Q1,Q2,Q3,Q4 = station insolations at the four successive times T1,T2,T3,T4.

The Langrangian fit was used to reduce the effect of transistory clouds over a short time frame.

D. PRECIPITABLE WATER VAPOR

Precipitable water vapor was computed from radiosonde soundings nearest to the pyrheliometric stations. The soundings were taken at 0000GMT and 1200GMT starting at 0000GMT 16 July 1966, and continuing through 0000GMT 20 July 1966. 16 levels were employed using the surface as the bottom level and the 15 standard levels at whole multiples of 50 mb above the surface. Temperatures and relative humidities (RH) at these levels were extracted from the soundings and used to compute water vapor mixing ratios at the indicated levels in the vertical. The computation

of q was facilitated, with RH known, by use of the Goff-Gratch (cf., List, 1958, p. 350) formulation of the saturation vapor pressure

$$\log_{10} e_w = -7.90298(T_s/T-1)+5.02809 \log_{10}(T_s/T)- 1.3816 \times 10^{-7}(10^{11.344(1-T/T_s)}-1) + 8.1328 * 10^{-3} * (10^{-3.49149(T_s/T-1)}-1) + \log_{10} e_{ws} \quad (12)$$

where

e_w = saturation vapor pressure over a plane surface of pure ordinary liquid water.

T = absolute temperature (^oK).

T_s = steam point temperature (373.16^oK).

e_{ws} = saturation pressure of pure liquid water at steam point temperature (1 standard atmosphere = 1013.246 mb).

Following the use of Eq. (12), the value of q is given by:

$$q = 621.97 \frac{e}{p-e} = 621.97(RH)e_w \over p-(RH)e_w \quad (13)$$

Then, precipitable water vapor is found from the mixing ratio integration

$$U = \frac{1000}{g}\int_{P_{sfc}}^{300} qdp \quad (14)$$

For the times on 16 July 1966 through 19 July 1966 a linear interpolation scheme between the 1200 and 0000GMT soundings was used to establish the precipitable water vapor at the effective time of satellite scan at each station.

More specific examples of the calculations performed in order to relate the satellite reflectance, and simultaneous station-transmittance through a physical relationship are detailed in Section III.

III. DATA PROCESSING

A. THE SOLAR-INSOLATION MODEL

In Section II, a general description was given of the data-collection problem at each pyrheliometric station at the effective time of the satellite scan. The immediate objective of the data-analysis corresponding to each station-observation was to solve the solar-insolation budget equation for the atmospheric absorptivity.

FIGURE 6

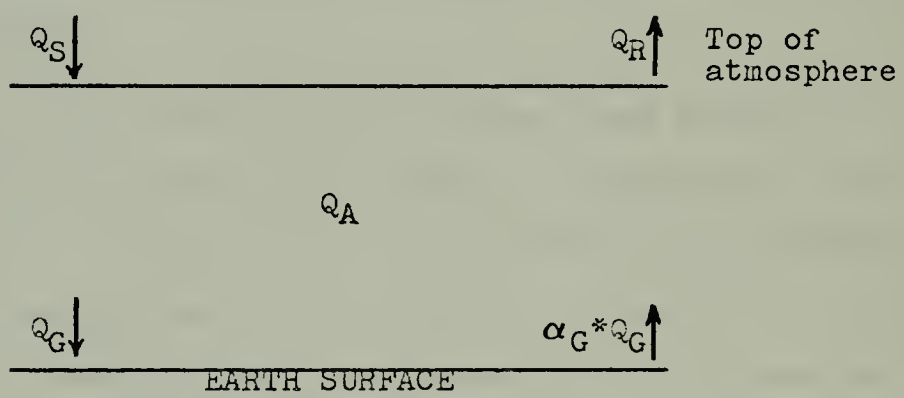

Figure 6. The solar-insolation model over a pyrheliometric station. See Eq. 15 and following for explanation of symbols.

Fig. 6 shows an insolation model after Fritz et al. (1964) and Hanson et al. (1967) which illustrates the terms involved in the solar-insolation budget at a satellite scan-time for a given pyrheliometric station. These terms are:

$$Q_S = S(r_m/r)^2 \cos Z \qquad (15)$$

Q_S = incident extraterrestial insolation based upon a solar constant S of 2.00 langleys min^{-1} (Q_S is the denominator of Eq. 5).

Q_G = pyrheliometric value of the insolation at the station interpolated to the true solar time (Eq. 8) of the satellite scan, according to Eq. 11.

Q_R = RQ_S, which is the reflected insolation at the station computed using the space-interpolated reflectance $R(I+\Delta I, J+\Delta J)$ of Eq. 10.

Q_A = absorbed insolation in the atmospheric column above the station.

α_G = surface albedo of the earth in the vicinity of the station.

The midsummer values of α_G were taken from a North American atlas reproduced here as Fig. 7 (prepared by Kung et al., 1964). The term $1-\alpha_G$ is the fractional absorption of the incident insolation Q_G, at earth. At each of the 47 pyrheliometer stations used, the atlas value of α_G has been listed next to the station coordinates (Appendix A).

The insolation-budget equation then according to Hanson et al. (1967) becomes:

$$Q_S = Q_R + Q_A + Q_G\ (1-\alpha_G) \qquad (16)$$

If each term of (16) is divided by Q_S, the equation may be rewritten as

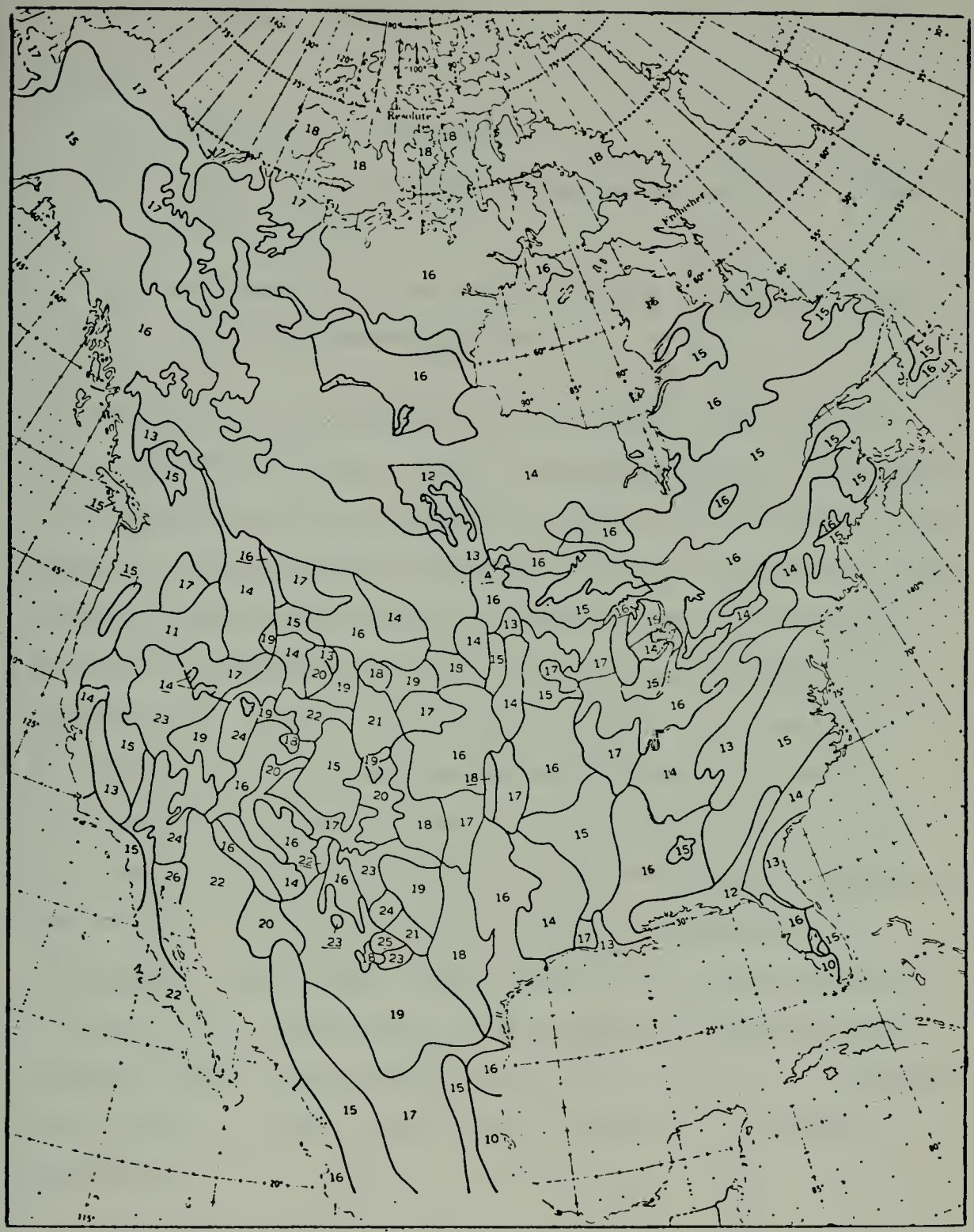

Figure 7 - Summer surface albedo map for North America (after Kung et al., 1964)

$$q_A = 1 - q_R - q_G\,(1-\alpha_G) \qquad (17)$$

where:

q_A = atmospheric absorptivity.

q_R = Q_R/Q_S is the computed reflectance using the NIMBUS II data-maps.

q_G = atmospheric transmissivity Q_G/Q_S as inferred from the pyrheliometer reading.

The parameter α_G was taken from the summer mean reflectance maps of Kung et al. (1964) for each station, and assumed constant during the NIMBUS II period 15-19 July 1966, although α_G varied from station to station in accordance with varying terrain and vegetation characteristics. The use of the α_G in connection with Eq. 17 was considered valid by Hanson et al. (1967) both in clear and partly cloudy sky conditions, and this same approximation is made here in reference to the computation of q_A in conditions of mixed cloudiness. An attempt is made in the subsequent regression analysis to isolate that part of q_A which depends upon cloudiness. Statistical specification of q_A similar to that of Hanson will be performed here using the simultaneously observed and/or calculated values of q_R, q_G, and α_G during the period 15-19 July 1966, with q_R measured by NIMBUS II satellite.

B. DATA TABULATIONS

For present tabulation purposes, the 47 insolation stations were assigned arbitrary station numbers 1, 2, ..., 47

TABLE I. TYPICAL SET OF INSOLATIONAL AND RELATED DATA AT PYRHELIOMETER STATIONS AT THE EFFECTIVE TIME OF THE NIMBUS II SCAN ON 17 JULY 1966

	Station No.	Extra-terrest Q_S, ly min^{-1}	Re-flected Q_R	Pyrhel-iometer Q_G	Absorbed (Air) Q_A	Precip Water Vapor U, gm cm^{-2}	Zenith Path SEC Z
	1	1.7790	0.6398	0.8319	0.4404	4.8232	1.0883
	2	1.8857	0.2711	1.3564	0.4210	4.5175	1.0267
	3	1.9189	0.3262	1.6974	0.1500	4.3973	1.0089
	4	1.7939	0.3243	1.4725	0.2328	4.4853	1.0792
	5	1.8884	0.7836	0.6680	0.5236	4.3882	1.0252
	6	1.8381	0.6659	0.6116	0.6461	4.3088	1.0533
	7	1.7782	0.3921	1.0544	0.5004	3.0089	1.0887
	8	1.7949	0.3647	1.1184	0.5130	2.6633	1.0786
	9	1.6741	0.2470	1.2202	0.3778	1.8045	1.1565
	10	1.7562	0.3273	1.1706	0.4573	2.2867	1.1024
	11	1.8971	0.4945	1.1978	0.4324	2.4511	1.0205
	12	1.8742	0.4056	1.6545	0.1782	2.1694	1.0330
	13	1.8047	0.3676	1.3676	0.3294	1.3708	1.0727
	14	1.8233	0.2287	1.3959	0.4080	2.1878	1.0618
	15	1.8660	0.3730	1.2186	0.5424	3.2688	1.0376
	16	1.8013	0.2279	1.3395	0.4348	1.3032	1.0748
P	17	1.6696	0.5659	-0.0474	1.1439	3.0095	1.1596
	18	1.7226	0.3008	1.1724	0.4487	1.5689	1.1238
	19	1.7201	0.2449	1.3934	0.3048	1.6416	1.1255
A	20	1.6415	0.5903	1.3108	-0.0499	1.6987	1.1794
	21	1.7945	0.3556	1.4354	0.1901	1.6033	1.0789
	22	1.8787	1.0111	0.2224	0.6764	4.5055	1.0305
	23	1.7861	0.3806	1.2782	0.3191	2.4676	1.0839
	24	1.7012	0.2461	1.0973	0.5225	1.4247	1.1380
	25	1.7691	0.3044	1.2806	0.3762	1.5437	1.0943
	26	1.7277	0.3217	1.3567	0.2528	3.1032	1.1206
	27	1.5645	0.5559	0.3864	0.6763	2.2638	1.2375
A	28	1.4358	0.7002	1.0219	-0.1330	2.1568	1.3484
	29	1.6297	0.5130	1.1258	0.1598	1.6994	1.1879
	30	1.5447	0.4654	1.0314	0.2027	2.2699	1.2533
	31	1.6977	0.2495	1.2607	0.3766	1.8045	1.1404
	32	1.5499	0.4177	1.0461	0.2535	2.1985	1.2491
	33	1.7278	0.2937	1.2433	0.3648	1.4729	1.1204
	34	1.7287	0.2173	1.2437	0.4666	1.3883	1.1199
	35	1.6254	0.5605	0.4457	0.6861	3.0243	1.1910
	36	1.7199	0.2183	1.1793	0.4992	1.9092	1.1256
	37	1.6432	0.2796	1.2288	0.3315	2.1046	1.1781
	38	1.6118	0.6234	0.7737	0.3308	2.8319	1.2012
	39	1.6971	0.3342	1.1203	0.4218	2.1268	1.1408
P	40	1.6605	0.1193	1.6500	0.1553	1.4620	1.1659
P	41	1.6035	0.3091	1.6500	-0.1081	1.5630	1.2074
	42	1.6532	0.5877	1.7551	0.4311	1.5231	1.1711
	43	1.6297	0.2803	1.1822	0.3445	1.6260	1.1879
	44	1.7255	0.2697	1.2719	0.3620	1.4731	1.1220
	45	1.7255	0.2697	1.2948	0.3423	1.4731	1.1220
	46	1.6361	0.4925	0.9245	0.3671	1.6994	1.1833
	47	1.6180	0.6268	0.6268	0.4459	3.1851	1.1966

(see Appendix A, for station names, code and geographical coordinates). Thus, for each station of Fig. 1, the values Q_S, Q_G, Q_R were computed using Eqs. 15, 11, 10; and Q_A was computed as the residual from Eq. 16. A typical set of insolation values obtained for each of the 47 stations on 17 July 1966 is listed in Table I.

The primary objective here at the outset was to obtain a statistical regression for the absorptivity q_A against an effective measure of the water vapor absorbing mass in the air column above the pyrheliometer station. For this purpose simultaneous values of precipitable water vapor U and of sec Z were also listed in Table I.

The complete set of raw data to be used for this regression analysis is tabulated in Appendix B. There were in all 47 X 5 = 235 simultaneous values of the variables Q_S, Q_R, Q_G, Q_A, α_G as these have been defined above in Eq. 15 and in the lines just following Eq. 15. Of the 188 reports listing the dependent sample-data taken from days 2 through 5 (July 15, ..., 19th, inclusive) in Appendix B, it was found that eight cases had missing pyrheliometer values at the solar hour adjacent to the effective time of the NIMBUS scan, and thus led to unreasonable transmissivities. These pyrheliometer-associated inconsistencies in the data field were denoted by the code symbol P.

On the other hand, for days two through five, there also occurred six cases of negative Q_A after Eq. 16 was applied,

which were also physically impossible. All cases for which Q_A were negative were coded by the symbol A (negative absorptivity). Hence the remaining sample of 174 data sets from days two through five were used in the further screening-analyses to be described in Section III (C). For an illustration of the initial screening involving data-deletions of code P and A, reference should be made to Table I in the column listing the pyrheliometer station number. Secondary data-screens which lead to further data-exclusions based upon statistical tests, are utilized for additional deletions of data cases based upon improbable extreme values of

$$q_A,\ q_G \text{ and } q_R$$

These tests are essentially based upon the requirements:

$$q_A = 1 - q_G\ (1-\alpha_G) - q_R \begin{matrix} < q_A(MAX) \\ > q_A(MIN) \end{matrix} \qquad (18)$$

Here the values of $q_A(MIN)$ and $q_A(MAX)$ are indicated by empirical evidence to be discussed in Section III (C).

C. APPLICATION OF A DATA-LIMIT SCREEN

1. General Considerations

Hanson et al. (1967) developed a best-fit regression for q_A using data based upon TIROS reflectances, and an empirically-determined measure M_W of the water vapor absorber mass. Hanson found the most effective definition of M_W, which led to the highest linear correlation of q_A with M_W, to be:

$$M_W = (U \sec Z)^{\frac{1}{2}} \ln (U \sec Z) \qquad (19)$$

The specific form of Hanson's regression was:

$$q_A = 0.096 + 0.045\, M_W \qquad (20)$$

which in turn was optimal in yielding the highest value of the correlation coefficient R between q_A and M_W

$$R\,(q_A, M_W) = \text{Maximum}$$

Here M_W of (19) was one of many possible functions of U sec Z having the empirical form of an absorptivity (see Fig. 8).

Application of the BIMED 02R statistical program (on file in the Program Library of the W. R. Church Computer Center of the Naval Postgraduate School) to the dependent sample of 174 data-cases from days two through five, was made in order to generate the least-squares best-fit between

(a) q_A and M_W

(b) q_G and M_W

(c) q_R and M_W

The most useful <u>immediate results</u> obtained here were listings of sample means and standard deviations (S.D.) of each variable under consideration, (as well as listings of the 174 values) of q_A, q_G and q_R (see Table II).

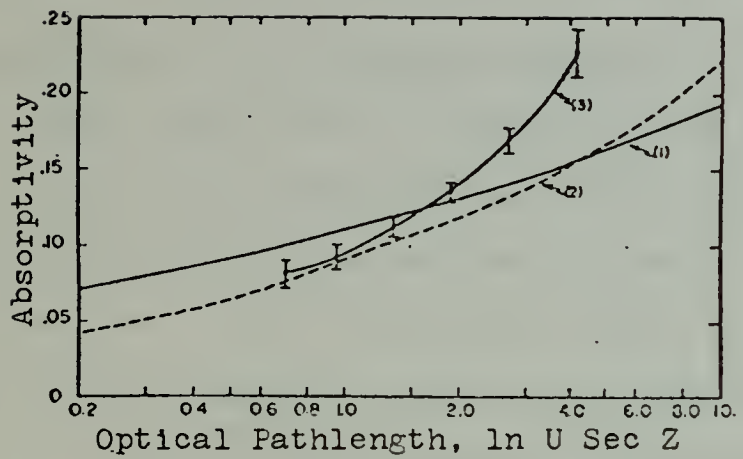

Figure 8. Absorptivity of solar radiation in the atmosphere as a function of optical pathlength, ln U Sec Z. Curve (1) is the absorptivity in a clear atmosphere by H_2O, CO_2, and O_2, from Yamamoto (1962). Curve (2) is the absorptivity in the clear atmosphere by H_2O only, from Houghton (1954). Curve (3) is the absorptivity in the atmosphere over the United States with mixed cloudiness, based on the Hanson's 1967 study. Vertical bars indicate the most probable error at the abscissa value.

TABLE II. Statistics Pertaining to q_A, q_G, q_R

	Mean	S.D.	Range
q_A	0.2290	0.0943	0.0026 to 0.6192
q_G	0.6308	0.1964	0.0747 to 0.9594
q_R	0.2388	0.1127	0.0916 to 0.6406 = q_R(MAX)

2. Consideration of Data-Exclusions on q_R

The listed range of the planetary albedo q_R in Appendix B is within the range of albedo values quoted in the literature (List, 1958) for various surfaces: cloud-tops, soil-types, etc. Hence no limiting range on the values of q_R found here were imposed on any of the data cases of this study, i.e., no data-case exclusions were made on the basis of q_R. This does not mean that q_R does not have a measurement error, but that its effect on upsetting the balance of Eq. 17 is not as great as the more unrealistic ranges of values associated with q_A and q_G.

3. Data-Exclusions Based on q_A

Because q_A was determined as a residual involving the two measured (but error-subject) quantities q_R and q_G, it was felt that some reasonable bounds would have to be applied to the range of q_A. Thus q_A(MIN) and q_A(MAX) values were established in accordance with 1% extreme-probability limits on both wings of a Gaussian distribution centered on

q_A(MEAN). From the statistics of Table II, it follows that the definition of:

$$q_A(\text{MIN}) = 0.2290 - 2.3267\ (0.0943) = 0.0096 \qquad (21)$$

$$q_A(\text{MAX}) = 0.2290 + 2.3267\ (0.0943) = 0.4484 \qquad (22)$$

The value of q_A(MIN) was relaxed to:

$$q_A(\text{MIN}) = 0.07 \qquad (23)$$

[cf., Fig. 8, after Hanson et al. (1967)]. With the limits established by Eqs. 22 and 23, there were six case-deletions due to small absorptivity-calculations

$$q_A < 0.07$$

and 4 case deletions due to unacceptably large q_A

$$q_A > 0.4484$$

These ten deletions are coded A MIN, A MAX in Appendix Table B. The codes MIN and MAX indicate that statistical-empirical considerations were involved in these q_A secondary-deletions.

4. Data-Exclusions based on q_G

Here two statistical relationships analogous to Eqs. 21, 22 for considering probable limits on q_G were set up:

$$q_G(\text{MIN}) = 0.6308 - 2.576\ (0.1964) = 0.1249 \qquad (24)$$

$$q_G(\text{MAX}) = 0.6308 + 2.576\ (0.1964) = 1.1367 \qquad (25)$$

The factors 2.576 in Eqs. 24, 25 correspond to limiting data-cases lying in a 0.5% rather than in a 1% Gaussian probability distribution wing. Here we are being slightly more cautious about rejecting extreme values of q_G than in the corresponding consideration of q_A. Finally Eq. 25 has been altered from an extreme transmissivity of 114% to 93% (i.e., 0.93). This follows in accordance with the minimum $q_A = 0.07$ of Eqs. 23 and 18 so that:

$$q_G(MAX) = 0.93 \qquad (26)$$

the upper limit exclusion Eq. 26 accounted for no data-case rejections, while the lower limit of Eq. 24 accounted for four data-case rejections. These cases are listed in Appendix Table B by the symbolism T MIN. The revised data-sample size for regression purposes now comprises 160 cases.

Actually the purpose of reducing the number of extreme data cases was to eliminate as much noise as possible from the regression analysis so that the physical-statistical relationships would stand out more clearly. It will be seen in Section IV that the data-screening process for elimination of extreme-cases did not improve the regression analysis markedly, after the initial reduction to the sample of 174 cases (based upon obviously missing and erroneous data) was achieved.

IV. THE REGRESSION RESULTS

A. THE REGRESSION ANALYSIS FOR q_A

Initially a least-squares fit analogous to that of Hanson (Eqs. 19, 20) was sought, using both the full sample-set of 174 cases, and the smaller sample-set of 160 cases after extreme-value limits had been applied to screen statistically for possible unreliable data. The regression method used was that of BIMED 02R (Dixon, 1970). Seven variables were listed on an IBM card for each data-case. Following are the variables listed for each case in Appendix Table B, namely:

$$Q_S,\ Q_R,\ Q_G,\ Q_A,\ U,\ \cos Z,\ \alpha_G$$

By means of transgeneration (an option of the BIMED series of programs), the fractions $q_A = Q_A/Q_S$, q_G, q_R were formed, as well as the water vapor mass M_W (Eq. 19) used by Hanson et al. (1967).

Two types of regression tests were run for both the raw-data and screened-data sample sets. These tests involved:

(1) q_A on M_W alone

(2) q_A on both M_W and q_R

The reason for performing the regression-test (2) is that it was observed that an above (below) normal q_A tended to occur with an above (below) normal q_R. In fact the correlation coefficient between q_A and q_R was $R(q_A, q_R) = 0.335$.

More specifically, an increase in q_R is, in general, associated with an increase of cloud cover, so that the inclusion of q_R as a predictor for q_A should indicate at least partially an effect of the cloud cover on q_A. Moreover with the NOAA satellite scanning radiometer readout available at Fleet Weather Centrals, values of q_R ought to be as readily accessible as the radiosonde data used for the M_W computation.

The two regression tests on the raw and statistically-screened data sets led to the following regression equations and associated correlation coefficients R.

Test 1, sample size n = 174 (raw data test):

$$q_A = 0.1983 + 0.0188\ M_W \qquad (27)$$

$$R = 0.1807$$

Test 1, sample size n = 160 (screened data):

$$q_A = 0.1978 + 0.0189\ M_W \qquad (28)$$

$$R = 0.2206$$

Test 2, sample size n = 174 (raw data):

$$q_A = 0.1649 + 0.1880\ q_R + 0.0118\ M_W \qquad (29)$$

$$R = 0.2802$$

Test 2, sample size n = 160 (screened data):

$$q_A = 0.1605 + 0.2162\ q_R + 0.0111\ M_W \qquad (30)$$

$$R = 0.3567$$

Since the correlation coefficient squared (R^2) is the measure of the explained fraction of the variance introduced by the regression technique, it is clear that q_A is not well specified by either M_W and/or by q_R in spite of evidence to the contrary by Hanson et al. (1967). The most significant correlation for q_A of the set of Eqs. 27, 28, 29, 30, is that involving both q_R and M_W as predictands with statistically screened data. The mean statistics which relate to the four tests just cited are summarized in Table III. The mean standard error of estimate for the best case (line 4) in Table III was S.E. = 0.0715.

The relatively large standard error which remains after the regression tests (Table III), seems to be due to the computational formula for q_A of (17),

$$q_A = 1 - q_R - (1-\alpha_G)q_G \qquad (17)$$

This equation has been used with <u>partly cloudy</u> to <u>cloudy</u> skies, when q_G has already been reduced by the cloudiness associated with the large reflectance q_R. However, in these cloudy cases, the multiplicative reduction of the q_G term of (17) by the factor $(1-\alpha_G)$ gives a positive bias to the computation of q_A which shows up in the predominance of large positive residuals remaining after application of the regressions, Eqs. 27, 28, 29, 30.

Table III

Regression Statistics for
Tests of (1) q_A on M_W; (2) q_A on M_W, q_R

Test	Sample Size	Mean q_A	Standard Deviation $\sigma(q_A)$	Corr. Coeff.	% Expl. Variance	Std. Err. of Est.
(1) q_A on M_W	174	0.2290	0.0943	0.1807	3.27	0.0931
(1) q_A on M_W	160	0.2275	0.0760	0.2206	4.87	0.0744
(2) q_A on M_W, q_R	174	0.2290	0.0943	0.2802	7.85	0.0911
(2) q_A on M_W, q_R	160	0.2275	0.0760	0.3567	12.72	0.0715

B. A REGRESSION ANALYSIS FOR q_G

The relatively weak statistical specification of q_A was due in part to improper accounting for earth-surface absorption term in Eq. 17 when clouds were present. However q_G is a measured parameter, which is related to q_A through

$$\text{Clear case:} \quad q_G = \frac{1-q_R-q_A}{1-\alpha_G} \tag{31}$$

$$\text{Overcast case:} \quad q_G = 1-q_R-q_A \tag{32}$$

Hence, since the computational error in determining q_A tends to obscure the statistical regression of q_A on M_W and q_R. Eqs. 31, 32 suggest that such a statistical relationship might be contained in a regression of the transmissivity q_G on M_W and q_R in view of the functional relationships (31), (32) between q_G and q_A. There seems to be a greater likelihood of a significant regression for q_G than for q_A in view of the fact that q_G is directly measured. The assumption of a significant regression of the type just described is the hypothesis of subsection IV (B).

In the statistical tests to be conducted here, q_G is established as the predictand in a set of regression tests for

(1) q_G on M_W alone,

(2) q_G on M_W and q_R.

These tests then led to the following regression results in Eqs. 33, 34, 35, 36 which are the analogs of Eqs. 27, 28, 29, 30, respectively. The associated regression statistics are listed in Table IV.

Table IV

Regression Statistics for
Tests of (1) q_G on M_W; (2) q_G on M_W and q_R

Test	Sample Size	Mean q_G	Std. Dev. $\sigma(q_G)$	Corr. Coeff.	% Expl. Variance	Std. Err. of Est.
(1) q_G on M_W	174	0.6308	0.1964	0.3124	9.77	0.1871
(1) q_G on M_W	160	0.6429	0.1752	0.3369	11.35	0.1654
(2) q_G on M_W, q_R	174	0.6308	0.1964	0.8236	67.83	0.1120
(2) q_G on M_W, q_R	160	0.6429	0.1752	0.8679	75.32	0.0876

Test 1, sample size n = 174 (raw data):

$$q_G = 0.74141 - 0.0677M_W \qquad (33)$$

$$R = 0.3124$$

Test 1, sample size n = 160 (screened data):

$$q_G = 0.74743 - 0.0665M_W \qquad (34)$$

$$R = 0.3369$$

Test 2, sample size n = 174 (raw data):

$$q_G = 0.9887 - 1.3927q_R - 0.0155M_W \qquad (35)$$

$$R = 0.8236$$

Test 2, sample size n = 160 (screened data):

$$q_G = 0.99252 - 1.42078q_R - 0.01509M_W \qquad (36)$$

$$R = 0.8679$$

Note the relatively high correlation coefficients in the Test (2) case in the specification of q_G in terms of both M_W and q_R. The results seem to be slightly better in the case of filtered data (sample size of 160), where the standard error of estimate of q_G is 0.0876 compared to 0.1120 in the case of the raw data.

In Table IV, the lower values of the correlation of q_G on M_W alone suggests that the q_G estimations developed from (33), (34) will not be as useful as those derived from (35), (36). This will be further explained in Subsection (C).

C. TESTS ON INDEPENDENT DATA-SAMPLES

In Sections IV (A) and (B), four sets of regression equations for both q_A and q_G were statistically deduced

based upon the dependent-data samples of 174 and 160 cases, respectively (termed the raw-data and statistically-screened samples, respectively).

The regression equations so derived were of the form:

$$\hat{q}_A = A_0 + A_1 q_R + A_2 M_W \tag{37}$$

$$\hat{q}_G = B_0 + B_1 q_R + B_2 M_W \tag{38}$$

and represent approximations to the observed or measured q_A, q_G. In Eqs. 27 and 28, the special case

$$A_1 = 0$$

was enforced, while in Eqs. 33, 34, we required

$$B_1 = 0$$

Eqs. 37, 38 with $A_1 = 0$, $B_1 = 0$, respectively were termed the Test 1 regressions, while $A_1 \neq 0$, $B_1 \neq 0$, have been termed the Test 2 regressions.

The generating formulas of Eqs. 37 and 38 may be written in the matrix-product notation:

$$\hat{q}_A = (A_0, A_1, A_2) \begin{pmatrix} 1 \\ q_R \\ M_W \end{pmatrix} \tag{39}$$

$$\hat{q}_G = (B_0, B_1, B_2) \begin{pmatrix} 1 \\ q_R \\ M_W \end{pmatrix} \tag{40}$$

Here A_0, A_1, A_2 are listed in Eqs. 37, 38, 39, 40 and B_0, B_1, B_2 are listed in (33, ..., 36).

Table V

Independent Sample Regression Tests

(a) Raw-Data Sample, n=44

Predictand	Means	Standard Dev. $\sigma(q)$	Standard Error	Correlation Coefficient
q_A	$\bar{q}_A$=0.2179	0.0882	------	----------
	$\bar{\hat{q}}_A$=0.2281	0.0263	0.0860	R=0.2652, by Eq. 27
	$\bar{\hat{q}}_A$=0.2268	0.0290	0.0871	R=0.2155, by Eq. 29
q_G	$\bar{q}_G$=0.6575	0.1718	------	----------
	$\bar{\hat{q}}_G$=0.6372	0.0805	0.1688	R=0.2387, by Eq. 33
	$\bar{\hat{q}}_G$=0.6465	0.1544	0.1073	R=0.7868, by Eq. 35*

(b) Screened Data, n=41

q_A	$\bar{q}_A$=0.2124	0.0688	------	----------
	$\bar{\hat{q}}_A$=0.2253	0.0198	0.0688	R=0.0551, by Eq. 28
	$\bar{\hat{q}}_A$=0.2240	0.0246	0.0688	R=0.0975, by Eq. 30
q_G	$\bar{q}_G$=0.6745	0.1467	------	----------
	$\bar{\hat{q}}_G$=0.6508	0.0696	0.1467	R=0.0865, by Eq. 34
	$\bar{\hat{q}}_G$=0.6588	0.1383	0.0882	R=0.8048, by Eq. 36*

For the independent test, the simultaneous samples $(q_A, \hat{q}_A)$ and $(q_G, \hat{q}_G)$ from day 1 were used. For the test on the raw-data independent sample of day one, the four specific coefficient sets of A_0, A_1, A_2 and B_0, B_1, B_2 of Eqs. 27, 29, 33, 35 were used. For the test on the screened-data independent sample of day one, the four coefficient sets of Eqs. 28, 30, 34, 36, respectively were used. The regression results for the eight combinations of the one-predictor and two-predictor formulas for q_A and q_G are shown in Table V for both the raw and screened independent sample tests.

Table V shows that the use of screened data in place of raw data caused a decrease in the standard deviation of the predictand by eliminating some of the extreme values. Moreover the correlation coefficients:

$$R(q_A, \hat{q}_A),\ R(q_G, \hat{q}_G)$$

decreased from the raw to the screened cases when the listed values of the correlation coefficients of the initial specification Eqs. 27, 28, 29, 30, 33, 34 were small (in the range .2 to .35). However the two key results which stand out in Table V are those corresponding to the use of specifying Eqs. 35, 36 (which gave R = 0.7868 and 0.8048, respectively), denoted by an asterisk superscript in Table V.

These two key results indicate that the transmissivity-estimator $\hat{q}_G$ expressed by either Eq. 35 or 36 gives a significantly good specification for the pyrheliometric observation of q_G.

The interpretation of the correlation coefficients R in the two cases noted in Table V may be seen from the standard statistical formula:

$$R^2 = \frac{\text{Mean square explained by Regression}}{\text{Mean square of predictand}} \qquad (41)$$

$$= \frac{\sigma_q^{\,2} - (SE)^2}{\sigma_q^{\,2}}$$

Thus by use of Eq. 35, the standard error is 0.1073, whereas the original standard deviation is 0.1718. Likewise by use of Eq. 36 the standard error is 0.0882 compared to the original standard deviation of 0.1467, as summarized by Table V.

Actually, there has been no appreciable significant change in the fractional part of explained variance by (35) versus (36). Moreover the process of providing screening limits is very laborious if it provides no significant improvement in the fractional explained variance (right side of Eq. 41).

D. ERROR CONSIDERATIONS

As has already been noted, there is a substantial standard deviation in q_G (0.1964 in the case of raw data, 0.1752 in the case of screened). A substantial part of this error is due to initial calibration of the Eppley pyrheliometers, ranging from 3.5 to 10.5%, Hanson et al. (1972). While such errors may be partially accounted for and correction

factors applied, the nature of the correction process was not known until the present study was completed. It is likely that a sizeable fraction of the standard error of estimate of q_G listed in the last line of Table IV is due to the pyrheliometer calibration error.

Another minor source of instrumental error is that due to the necessity of interpolation of q_G in time between tabulated hourly solar transmission increments. The non-availability of detailed digitized records of the pyrheliometer and satellite reflectance data both on a sensitive time scale was another error-source in this study since short-term cloud variations of a period less than a half-hour would have been related to the short term variabilities of q_G and of q_R. Note that in this connection, our time-smoothed records of q_G and q_R were highly correlated, there being a correlation coefficient $R\ (q_G, q_R) = -0.821$.

As mentioned earlier in connection with the effect of cloud-cover on the computation of q_G (Eqs. 31, 32), two different formulas apply in the clear and overcast cases for the solar-insolation budget as accounted for at the pyrheliometer. Failure to explicitly account for the amount of cloud-cover has biased the computation of q_A in the sense of increasing the value of the latter by up to 15% (that is, by the factor $CL/(1-\alpha_G)$ in Eq. 31, where CL is the cloud-cover). A discussion for the systematic inclusion of the cloud cover parameter for improved specification of q_A and q_G is given in Section V.

V. RECOMMENDATIONS AND CONCLUSIONS

As deduced from this study, the insolational budgetary model of Eqs. 17 and 31 gave q_A values biased towards high values. This was due to the failure to account for the effects of cloud cover properly, as shown for the overcast case in Eq. 32. The combination of Eqs. 31, 32 show that for some intermediate cloud-cover state CL, the properly weighted form of these two equations leads to

$$q_A = 1 - q_R - q_G \left[1 - \alpha_G (1-CL)\right] = 0 \qquad (42)$$

In Eq. 42, the term involving α_G is the fractional insolation which the cloud-openings (1-CL) permit to escape to space.

In this study, CL was not known and was assumed zero, as was also done by Hanson et al. (1967) and Fritz et al. (1964). However, recent studies by Downey et al. (1972) showed that q_R is highly correlated with CL, as indicated by the following summary of his results (based on NIMBUS III observations).

Correlation coefficients $R(q_R, CL)$ by periods 1969-70.

May 16-31	Aug. 1-15	Oct. 3-17	21 Jan-3 Feb. 1970
0.64	0.78	0.78	0.85

With results of this type, combined with satellite measurements of window-channel temperatures as well, seasonal

regressions of some physically realistic form should be fitted to the observed cloud-coverage. The objective is to obtain a highly specifying representation for CL of form

$$CL = F(q_R, T_{BB}) \tag{43}$$

where F is the desired statistically-generated function of the indicated variables.

A seasonal variation may be built into the function F by making F dependent upon sec Z, where Z = zenith angle.

Finally the observed values of q_G which are used in connection with the solution of (42) for q_A should be carefully corrected for initial calibration and pyrheliometer degradation errors after the procedure recommended by Hanson et al. (1972).

APPENDIX TABLE A

NORTH AMERICAN PYRHELIOMETER STATION INFORMATION

Stat. No.	Code	Name	Index	Lat.	Long.	Albedo
1	AA	Fort Worth, Texas	72259	32-50	97-03	16
2	AB	Apalachicola, Fla.	220	29-44	84-59	12
3	AC	Miami, Florida	202	25-48	80-16	15
4	AD	Brownsville, Texas	250	25-54	97-26	16
5	AE	Charleston, S.C.	208	32-54	80-02	13
6	AF	Nashville, Tenn.	327	36-07	86-41	14
7	AG	Columbia, Mo.	445	38-58	92-22	16
8	AH	Dodge City, Kansas	451	37-46	99-58	18
9	AI	Caribou, Maine	712	46-52	68-01	14
10	AJ	Madison, Wisc.	641	43-08	89-20	17
	RS	Green Bay, Wis.	645			
11	AK	El Paso, Texas	270	31-48	106-24	19
12	AL	Albuquerque, N.M.	365	35-03	106-37	22
13	AM	Ely, Nevada	486	39-17	114-51	19
14	AN	Los Angeles, Ca.	295	33-56	118-23	15
	RS	San Diego, Ca.	290			
15	AO	Phoenix, Ariz.	278	33-26	112-01	22
	RS	Tucson, Ariz.	274			
16	AP	Santa Maria, Ca.	394	34-54	120-27	15
	RS	Vandenburg, Ca.	393			
17	AQ	Bismark, N.D.	764	46-46	100-45	15
18	AR	Great Falls, Mont.	775	47-29	111-22	17
19	AS	Medford, Oregon	597	42-22	122-52	16
20	AT	Tacoma, Wash.		47-57	124-33	16
	RS	Tatoosh, Wash.	798			
21	AU	Fresno, Ca.	389	36-46	119-43	13
	RS	Oakland, Ca.	493			
22	AV	Cape Hatteras, N.C.	304	35-16	75-33	14
23	AW	Sterling, Va.		39-00	77-26	15
24	AX	Boston, Mass.	509	42-22	71-02	15
	RS	Nantucket, Mass.	506			
25	AY	New York, N.Y.	74486	40-39	73-47	15
26	AZ	Omaha, Nebr.	72553	41-22	96-03	15

Stat. No.	Code	Name	Index	Lat.	Long.	Albedo
27	CA	Beaverlodge CDA, Alta.		55-12	119-30	14
	RS	Prince George B.C.	72896			
28	CB	Churchill, Man.	913	58-45	90-05	15
29	CC	Departure Bay, B.C.		49-12	124-00	15
	RS	Tatoosh, Wash.	798			
30	CD	Edmonton, Alta.	74119	53-19	113-35	15
31	CE	Fredericton CDA, N.B.		45-52	66-32	15
	RS	Caribou, ME	72712			
32	CF	Goose A, (Nfld)	816	53-19	60-25	16
33	CG	Guelph OAC (Ont.)		43-36	80-18	14
	RS	Buffalo, N.Y.	528			
34	CH	Halifax, N.S.		44-53	63-31	16
	RS	Sable, ISC	600			
35	CI	Kapuskasing A. Ont.		49-25	82-28	15
	RS	Moosonee CDA, Ont.	836			
36	CJ	Kentville CDA N.S.		45-06	64-30	15
	RS	Portland, ME	606			
37	CK	Montreal, Qua.		45-30	73-42	16
	RS	Maniwaki, CDA, Que	722			
38	CL	Normandin, CDA, Que		48-54	72-36	15
	RS	Sept. Isles, CDA, Que	811			
39	CM	Ottawa NRC, Ont.		45-24	75-42	16
	RS	Maniwaki, CDA, Que	722			
40	CN	St. John's West,CDA,(Nfld)		47-37	52-45	16
	RS	Stephenville, (Nfld)	815			
41	CO	Suffield A, Alta.		50-16	111-11	15
	RS	Great Falls, Mont.	775			
42	CP	Summerland CDA, B.C.		49-36	119-42	16
	RS	Spokane, Wash.	785			
43	CQ	Swift Current CDA, Sask.		50-17	107-41	15
	RS	Glasgow, Mont.	768			
44	CR	Toronto, Ont.		43-43	79-14	14
	RS	Buffalo, N.Y.	528			
45	CS	Toronto Searborough, Ont.		43-43	79-14	14
	RS	Buffalo, N.Y.	528			
46	CT	Vancover UBC, B.C.		49-11	123-10	16
	RS	Tatoosh, Wash.	798			
47	CU	Winnipeg Int A. Man.		49-54	97-14	13
	RS	International Falls,Minn.	747			

APPENDIX B

Tables of observational data interpolated to the effective scan-time at each of the 47 stations used in this study, and for days 1, ..., 5, (July 15, ..., 19, respectively).

The symbols Q_S, Q_R, Q_G, Q_A, α_G are as defined in Eq. 15 and in the paragraph which immediately follows this equation. The symbol U denotes the precipitable water vapor at the station and CZ is the cosine of the zenith angle at the effective time of the observation.

DELETE CODE symbols P and A indicate inconsistent transmission and absorption values, respectively, and these data-cases were not used. All other codes, such as A MAX, A MIN, T MIN express the occurrence of statistically improbable values, which cases were used in a secondary data-cases (Sec. III. (C)).

DATA FROM 15 JULY 1966

DAY	STAT	QS	QR	QG	QA	U	CZ	AG	DELETE CODE
1	1	1.8882	0.3428	1.5075	0.2791	4.9250	0.9753	0.1600	
1	2	1.8106	0.2272	0.8125	0.8684	4.4555	0.9352	0.1200	A MAX
1	3	1.8608	0.2150	1.2630	0.5723	4.0919	0.9612	0.1500	
1	4	1.9174	0.2712	1.5549	0.3402	4.1116	0.9904	0.1600	
1	5	1.8373	0.2700	1.2024	0.5213	15.7522	0.9490	0.1300	P
1	6	1.7630	0.3461	1.1852	0.3975	4.8400	0.9106	0.1400	
1	7	1.7959	0.6623	0.9030	0.3751	4.4345	0.9276	0.1600	
1	8	1.8406	0.5340	1.2044	0.3189	2.8051	0.9507	0.1800	
1	9	1.6887	0.4893	0.7286	0.5727	1.7243	0.8722	0.1400	
1	10	1.6792	0.3055	1.2436	0.3416	1.6213	0.8674	0.1700	
1	11	1.8545	0.4549	1.5045	0.1810	2.0278	0.9579	0.1900	
1	12	1.8269	0.4296	1.5882	0.1586	3.0699	0.9437	0.2200	
1	13	1.7279	0.3669	1.3698	0.2514	0.9352	0.8925	0.1900	
1	14	1.8526	0.3136	1.4474	0.3087	2.8593	0.9569	0.1500	
1	15	1.7936	0.4149	1.1547	0.4780	3.3418	0.9265	0.2200	
1	16	1.8813	0.4686	1.3992	0.2234	1.4571	0.9717	0.1500	
1	17	1.6908	0.5959	0.9303	0.3041	2.4923	0.8733	0.1500	
1	18	1.6701	0.2460	1.1271	0.4886	1.8121	0.8627	0.1700	
1	19	1.7619	0.3140	1.4109	0.2628	1.5175	0.9101	0.1600	
1	20	1.6804	0.3494	0.8058	0.6541	1.5016	0.8680	0.1600	
1	21	1.8247	0.3515	1.4469	0.2144	1.0191	0.9425	0.1300	
1	22	1.8498	0.5062	0.9736	0.5063	5.4871	0.9555	0.1400	
1	23	1.8087	1.0925	0.4028	0.3738	2.2825	0.9342	0.1500	
1	24	1.6971	0.3145	1.3140	0.2657	1.9185	0.8766	0.1500	
1	25	1.8089	0.8703	1.2631	-0.1351	2.1803	0.9343	0.1500	A
1	26	1.7662	0.9658	0.1267	0.6927	3.8785	0.9123	0.1500	T MIN
1	27	1.5392	0.3127	1.0919	0.2875	2.3963	0.7950	0.1400	
1	28	1.4560	0.2207	1.1779	0.2340	2.6781	0.7520	0.1500	
1	29	1.6575	0.5827	1.2543	0.0086	1.5016	0.8562	0.1500	A MIN
1	30	1.5710	0.3306	0.9188	0.4594	2.4760	0.8115	0.1500	
1	31	1.7086	0.3742	1.2302	0.2887	1.7243	0.8825	0.1500	
1	32	1.5642	0.6933	0.5529	0.4065	1.5022	0.8080	0.1600	
1	33	1.7446	0.2561	1.3238	0.3500	1.3535	0.9011	0.1400	
1	34	1.6502	0.2061	1.2292	0.4115	1.3934	0.8523	0.1600	
1	35	1.6552	0.2654	1.2028	0.3474	1.7154	0.8549	0.1500	
1	36	1.7151	0.2277	1.3307	0.3582	1.3487	0.8859	0.1500	
1	37	1.7511	0.2868	1.2430	0.4202	1.6961	0.9045	0.1600	
1	38	1.6644	0.4889	0.6200	0.6485	1.8277	0.8597	0.1500	
1	39	1.7454	0.2793	1.3109	0.3650	1.6961	0.9015	0.1600	
1	40	1.6969	0.3178	1.6500	-0.0070	0.9284	0.8765	0.1600	P
1	41	1.6326	0.2534	1.2198	0.3424	1.8121	0.8433	0.1500	
1	42	1.6513	0.3223	1.1969	0.3236	1.3633	0.8529	0.1600	
1	43	1.6531	0.2519	1.1876	0.3918	2.1755	0.8539	0.1500	
1	44	1.7486	0.2449	1.2992	0.3864	1.3535	0.9032	0.1400	
1	45	1.7486	0.2449	1.3679	0.3273	1.3535	0.9032	0.1400	
1	46	1.6564	0.5885	0.7725	0.4191	1.5016	0.8556	0.1600	
1	47	1.6371	0.3062	1.1502	0.3302	2.1556	0.8456	0.1300	

DATA FROM 16 JULY 1966

DAY	STAT	QS	QR	QG	QA	U	CZ	AG	DELETE CODE
2	1	1.8488	0.8080	0.5301	0.5955	4.6129	0.9549	0.1600	
2	2	1.9134	0.1753	1.3712	0.5314	4.3298	0.9883	0.1200	
2	3	1.9297	0.3005	1.3835	0.4532	4.5849	0.9967	0.1500	
2	4	1.8719	0.3637	1.6553	0.1176	4.7939	0.9669	0.1600	A MIN
2	5	1.8488	0.5854	0.4802	0.8456	4.7774	0.9550	0.1300	
2	6	1.8686	0.6371	0.0806	1.1622	5.2778	0.9652	0.1400	P
2	7	1.8259	0.5109	1.2655	0.2519	3.8085	0.9431	0.1600	
2	8	1.7949	0.4726	1.1846	0.3508	2.5805	0.9271	0.1800	
2	9	1.7222	0.2400	1.3411	0.3288	1.4029	0.8896	0.1400	
2	10	1.7298	0.2873	1.3339	0.3354	2.0737	0.8935	0.1700	
2	11	1.7743	0.3968	1.4538	0.1998	1.9732	0.9164	0.1900	
2	12	1.7554	0.4179	1.5076	0.1616	2.6347	0.9067	0.2200	
2	13	1.8367	0.4842	1.4074	0.2126	1.5308	0.9487	0.1900	
2	14	1.8717	0.2585	1.4375	0.3914	2.4869	0.9668	0.1500	
2	15	1.8916	0.4819	1.1459	0.5159	3.4390	0.9771	0.2200	
2	16	1.8561	0.3766	1.4072	0.2634	1.2346	0.9587	0.1500	
2	17	1.6937	0.2598	1.1958	0.4175	2.4074	0.8748	0.1500	
2	18	1.6626	0.2909	1.0707	0.4829	1.4265	0.8588	0.1700	
2	19	1.7753	0.3097	1.4022	0.2877	1.7028	0.9170	0.1600	
2	20	1.6963	0.5307	0.8328	0.4660	1.8042	0.8762	0.1600	
2	21	1.8449	0.3240	1.4705	0.2416	1.3561	0.9530	0.1300	
2	22	1.7914	0.7421	1.2443	-0.0208	4.5640	0.9253	0.1400	A
2	23	1.7477	0.2930	1.3391	0.3166	2.0401	0.9027	0.1500	
2	24	1.7625	0.2514	1.3229	0.3865	1.1574	0.9103	0.1500	
2	25	1.7617	0.2052	1.3503	0.4087	1.4906	0.9100	0.1500	
2	26	1.7856	0.5926	1.2579	0.1238	2.8728	0.9223	0.1500	A MIN
2	27	1.5129	0.3541	1.1331	0.1844	2.1910	0.7815	0.1400	
2	28	1.4347	0.2910	0.7682	0.4908	2.3367	0.7411	0.1500	
2	29	1.6805	0.6459	1.0902	0.1079	1.8042	0.8680	0.1500	A MIN
2	30	1.5482	0.7938	0.2785	0.5177	2.5557	0.7997	0.1500	
2	31	1.7416	0.2363	1.3403	0.3660	1.4024	0.8996	0.1500	
2	32	1.5499	0.7310	0.1865	0.6623	1.7213	0.8006	0.1600	T MIN
2	33	1.6829	0.2556	1.2589	0.3446	1.4655	0.8693	0.1400	
2	34	1.6981	0.1871	1.2729	0.4417	1.5519	0.8771	0.1600	
2	35	1.5920	0.3109	0.9549	0.4694	2.0746	0.8223	0.1500	
2	36	1.7591	0.1860	1.3818	0.3986	1.3674	0.9086	0.1500	
2	37	1.7097	0.2631	1.2166	0.4246	1.4759	0.8831	0.1600	
2	38	1.6706	0.3131	1.2354	0.3073	1.9883	0.8629	0.1500	
2	39	1.6971	0.2624	1.2698	0.3680	1.4759	0.8766	0.1600	
2	40	1.6394	0.1784	1.6500	0.0750	1.3350	0.8468	0.1600	P
2	41	1.6104	0.2729	1.1873	0.3283	1.4300	0.8318	0.1500	
2	42	1.6225	0.5097	0.6140	0.5970	1.5610	0.8381	0.1600	
2	43	1.5976	0.2728	1.1437	0.3528	2.1749	0.8252	0.1500	
2	44	1.6911	0.2371	1.2664	0.3649	1.4655	0.8735	0.1400	
2	45	1.6911	0.2371	1.2664	0.3649	1.4655	0.8735	0.1400	
2	46	1.6845	0.6884	0.7916	0.3311	1.8042	0.8701	0.1600	
2	47	1.6694	0.2666	1.2135	0.3469	1.9802	0.8623	0.1300	

DATA FROM 17 JULY 1966

DAY	STAT	QS	QR	QG	QA	U	CZ	AG	DELETE CODE
3	1	1.7790	0.6398	0.8319	0.4404	4.8232	0.9189	0.1600	
3	2	1.8857	0.2711	1.3564	0.4210	4.5175	0.9740	0.1200	
3	3	1.9189	0.3262	1.6974	0.1500	4.3973	0.9912	0.1500	
3	4	1.7939	0.3243	1.4725	0.2328	4.4853	0.9266	0.1600	
3	5	1.8884	0.7836	0.6680	0.5236	4.3882	0.9754	0.1300	
3	6	1.8381	0.6659	0.6116	0.6461	4.3088	0.9494	0.1400	
3	7	1.7782	0.3921	1.0544	0.5004	3.0089	0.9185	0.1600	
3	8	1.7949	0.3647	1.1184	0.5130	2.6633	0.9271	0.1800	
3	9	1.6741	0.2470	1.2202	0.3778	1.8045	0.8647	0.1400	
3	10	1.7562	0.3273	1.1706	0.4573	2.2867	0.9071	0.1700	
3	11	1.8971	0.4945	1.1978	0.4324	2.4511	0.9799	0.1900	
3	12	1.8742	0.4056	1.6544	0.1782	2.1694	0.9681	0.2200	
3	13	1.8047	0.3676	1.3670	0.3294	1.3708	0.9322	0.1900	
3	14	1.8233	0.2287	1.3959	0.4080	2.1878	0.9418	0.1500	
3	15	1.8660	0.3730	1.2186	0.5425	3.2688	0.9638	0.2200	
3	16	1.8013	0.2279	1.3395	0.4348	1.3032	0.9304	0.1500	
3	17	1.6695	0.5659	-0.0474	1.1439	3.0095	0.8624	0.1500	P
3	18	1.7226	0.3008	1.1724	0.4487	1.5689	0.8898	0.1700	
3	19	1.7201	0.2449	1.3934	0.3048	1.6416	0.8885	0.1600	
3	20	1.6415	0.5903	1.3108	-0.0499	1.6987	0.8479	0.1600	A
3	21	1.7945	0.3556	1.4354	0.1901	1.6033	0.9269	0.1300	
3	22	1.8788	1.0111	0.2224	0.6764	4.5055	0.9704	0.1400	T MIN
3	23	1.7861	0.3806	1.2782	0.3191	2.4676	0.9226	0.1500	
3	24	1.7012	0.2461	1.0973	0.5225	1.4247	0.8787	0.1500	
3	25	1.7691	0.3044	1.2806	0.3762	1.5437	0.9138	0.1500	
3	26	1.7277	0.3217	1.3567	0.2528	3.1032	0.8924	0.1500	
3	27	1.5645	0.5559	0.3864	0.6763	2.2638	0.8081	0.1400	
3	28	1.4358	0.7002	1.0219	-0.1330	2.1568	0.7416	0.1500	A
3	29	1.6297	0.5130	1.1258	0.1598	1.6994	0.8418	0.1500	
3	30	1.5447	0.4654	1.0314	0.2027	2.2700	0.7979	0.1500	
3	31	1.6977	0.2495	1.2607	0.3766	1.8045	0.8769	0.1500	
3	32	1.5499	0.4177	1.0461	0.2535	2.1985	0.8006	0.1600	
3	33	1.7278	0.2937	1.2433	0.3648	1.4729	0.8925	0.1400	
3	34	1.7287	0.2173	1.2437	0.4666	1.3883	0.8929	0.1600	
3	35	1.6254	0.5604	0.4457	0.6861	3.0243	0.8396	0.1500	
3	36	1.7199	0.2183	1.1793	0.4992	1.9092	0.8884	0.1500	
3	37	1.6432	0.2796	1.2288	0.3315	2.1046	0.8488	0.1600	
3	38	1.6118	0.6234	0.7737	0.3308	2.8319	0.8325	0.1500	
3	39	1.6971	0.3342	1.1203	0.4218	2.1268	0.8766	0.1600	
3	40	1.6605	0.1193	1.6500	0.1553	1.4620	0.8577	0.1600	P
3	41	1.6035	0.3091	1.6500	-0.1081	1.5630	0.8282	0.1500	P
3	42	1.6531	0.5877	0.7551	0.4311	1.5231	0.8539	0.1600	
3	43	1.6297	0.2803	1.1822	0.3445	1.6260	0.8418	0.1500	
3	44	1.7255	0.2697	1.2719	0.3620	1.4731	0.8913	0.1400	
3	45	1.7255	0.2697	1.2948	0.3423	1.4731	0.8913	0.1400	
3	46	1.6361	0.4925	0.9245	0.3671	1.6994	0.8451	0.1600	
3	47	1.6180	0.6268	0.6268	0.4459	3.1851	0.8357	0.1300	

DATA FROM 18 JULY 1966

DAY	STAT	QS	QR	QG	QA	U	CZ	AG	DELETE CODE
4	1	1.8927	0.3193	1.4168	0.3833	4.5941	0.9776	0.1600	
4	2	1.8262	0.2151	1.2829	0.4821	5.4077	0.9433	0.1200	
4	3	1.8748	0.2179	1.6331	0.2688	4.0976	0.9684	0.1500	
4	4	1.9229	0.2778	0.5411	1.1906	4.5387	0.9932	0.1600	A MAX
4	5	1.8498	0.2525	1.5330	0.2637	3.1349	0.9555	0.1300	
4	6	1.7784	0.5182	1.1495	0.2716	3.9204	0.9186	0.1400	
4	7	1.8043	0.3251	1.1407	0.5210	3.5328	0.9319	0.1600	
4	8	1.8467	0.3504	1.3663	0.3760	2.4363	0.9539	0.1800	
4	9	1.6981	0.5717	0.6730	0.5476	2.5782	0.8771	0.1400	
4	10	1.6958	0.3431	1.1649	0.3858	3.1652	0.8759	0.1700	
4	11	1.8604	0.4967	1.5140	0.1374	2.8001	0.9609	0.1900	
4	12	1.8387	0.4638	1.7133	0.0385	2.4422	0.9497	0.2200	A MIN
4	13	1.7446	0.3801	1.3399	0.2791	1.2850	0.9011	0.1900	
4	14	1.8526	0.2721	1.3799	0.4076	2.4903	0.9569	0.1500	
4	15	1.8098	0.3905	1.1420	0.5286	3.5054	0.9348	0.2200	
4	16	1.8458	0.3849	1.3822	0.2860	1.8411	0.9534	0.1500	
4	17	1.6974	0.4977	0.4955	0.7786	2.7285	0.8768	0.1500	
4	18	1.6822	0.2624	1.1655	0.4525	1.7660	0.8689	0.1700	
4	19	1.7646	0.2526	1.4320	0.3091	1.5203	0.9115	0.1600	
4	20	1.6767	0.8308	1.2514	-0.2053	2.0556	0.8661	0.1600	A
4	21	1.8238	0.3434	1.4388	0.2286	1.7731	0.9420	0.1300	
4	22	1.8576	0.1875	1.4513	0.4220	2.9462	0.9595	0.1400	
4	23	1.8173	0.3053	1.1973	0.4942	2.4793	0.9387	0.1500	
4	24	1.7588	0.2973	1.2168	0.4272	2.0334	0.9085	0.1500	
4	25	1.8153	0.2678	1.2922	0.4492	2.3460	0.9376	0.1500	
4	26	1.7747	0.3423	1.3434	0.2905	4.1466	0.9167	0.1500	
4	27	1.5118	0.3500	1.0699	0.2417	1.7488	0.7809	0.1400	
4	28	1.4676	0.1820	1.2671	0.2086	1.3702	0.7581	0.1500	
4	29	1.6594	0.9419	0.3993	0.3780	2.0562	0.8571	0.1500	
4	30	1.5826	0.2852	1.1474	0.3222	1.8272	0.8175	0.1500	
4	31	1.7123	0.5425	0.7346	0.5453	2.5663	0.8844	0.1500	
4	32	1.5764	0.6449	0.3705	0.6203	2.9701	0.8143	0.1600	
4	33	1.7541	0.5754	0.7745	0.5127	2.2182	0.9061	0.1400	
4	34	1.6656	0.1866	1.2224	0.4522	1.4754	0.8603	0.1600	
4	35	1.6656	0.7425	0.3993	0.5837	1.9995	0.8603	0.1500	
4	36	1.6540	0.1920	1.2155	0.4289	2.2105	0.8543	0.1500	
4	37	1.7163	0.7507	1.1938	-0.0372	3.2486	0.8865	0.1600	A
4	38	1.6653	0.6240	0.8400	0.3273	2.9773	0.8602	0.1500	
4	39	1.7517	0.9253	0.1923	0.6649	3.2734	0.9048	0.1600	T MIN
4	40	1.7045	0.1648	1.6500	0.1537	2.0870	0.8804	0.1600	P
4	41	1.6438	0.2764	1.2424	0.3114	1.7656	0.8491	0.1500	
4	42	1.6513	0.3037	1.2222	0.3210	1.4911	0.8529	0.1600	
4	43	1.6622	0.2790	1.1788	0.3813	2.2745	0.8586	0.1500	
4	44	1.7583	0.6552	0.8095	0.4069	2.2182	0.9082	0.1400	
4	45	1.7583	0.6552	0.7917	0.4222	2.2182	0.9082	0.1400	
4	46	1.6564	0.7731	0.3515	0.5881	2.0583	0.8556	0.1600	
4	47	1.6438	0.3798	1.0482	0.3521	2.3445	0.8491	0.1300	

DATA FROM 19 JULY 1966

DAY	STAT	QS	QR	QG	QA	U	CZ	AG	DELETE CODE
5	1	1.8591	0.3304	1.4887	0.2782	3.6989	0.9603	0.1600	
5	2	1.9151	0.3005	1.3621	0.4159	3.6362	0.9892	0.1200	
5	3	1.7965	0.2686	1.4175	0.3230	4.1265	0.9280	0.1500	
5	4	1.8836	0.3620	1.6581	0.1288	4.4379	0.9729	0.1600	A MIN
5	5	1.7793	0.3190	1.3370	0.2971	3.7573	0.9191	0.1300	
5	6	1.8710	0.8220	1.0846	0.1162	4.4312	0.9664	0.1400	A MIN
5	7	1.8325	0.7282	-0.0008	1.1050	4.8745	0.9466	0.1600	P
5	8	1.8063	0.5431	1.1452	0.3241	3.4179	0.9330	0.1800	
5	9	1.7294	0.9189	0.2693	0.5789	3.7119	0.8933	0.1400	
5	10	1.7553	0.3935	1.2321	0.3392	2.1728	0.9067	0.1700	
5	11	1.7914	0.4139	1.4203	0.2271	2.7737	0.9253	0.1900	
5	12	1.7734	0.4417	1.7014	0.0046	2.6827	0.9160	0.2200	A MIN
5	13	1.8004	0.3647	1.3826	0.3159	1.2488	0.9299	0.1900	
5	14	1.8777	0.3902	1.4130	0.2865	2.1101	0.9699	0.1500	
5	15	1.8931	0.6507	0.5669	0.8001	3.1681	0.9778	0.2200	
5	16	1.8634	0.3060	1.4064	0.3620	1.6468	0.9625	0.1500	
5	17	1.7046	0.2919	1.1822	0.4078	2.6825	0.8804	0.1500	
5	18	1.6914	0.2587	1.1779	0.4550	1.6734	0.8736	0.1700	
5	19	1.7831	0.2695	1.2606	0.4547	1.5840	0.9210	0.1600	
5	20	1.7041	0.2483	1.1375	0.5003	1.3723	0.8802	0.1600	
5	21	1.8515	0.3302	1.4400	0.2685	1.6670	0.9563	0.1300	
5	22	1.8065	0.2424	1.3452	0.4072	2.2323	0.9331	0.1400	
5	23	1.7632	0.7172	0.7941	0.3710	2.9744	0.9107	0.1500	
5	24	1.7726	0.4982	0.8194	0.5779	2.6637	0.9156	0.1500	
5	25	1.7752	0.3764	1.1834	0.3929	3.3273	0.9169	0.1500	
5	26	1.5281	0.6149	1.1957	-0.1032	3.3319	0.7893	0.1500	A
5	27	1.5486	0.7537	0.4937	0.3703	1.6468	0.7999	0.1400	
5	28	1.4713	0.1782	1.2540	0.2272	1.7273	0.7600	0.1500	
5	29	1.6884	0.4145	1.1125	0.3283	1.3719	0.8721	0.1500	
5	30	1.5817	0.2597	1.2588	0.2520	1.9707	0.8170	0.1500	
5	31	1.7480	0.5158	0.7135	0.6258	3.7122	0.9029	0.1500	
5	32	1.5812	0.4926	0.8704	0.3575	2.0733	0.8167	0.1600	
5	33	1.6949	0.6674	0.4883	0.6076	3.5935	0.8754	0.1400	
5	34	1.7278	0.4367	0.5615	0.8194	2.7785	0.8924	0.1600	A MAX
5	35	1.6075	0.2963	1.2044	0.2875	1.3049	0.8303	0.1500	
5	36	1.7272	0.3749	0.4985	0.9286	2.8835	0.8921	0.1500	A MAX
5	37	1.7209	1.1023	0.1285	0.5106	2.7011	0.8889	0.1600	T MIN
5	38	1.6803	0.2934	0.9796	0.5543	2.4600	0.8679	0.1500	
5	39	1.7096	0.9978	0.2683	0.4864	2.7011	0.8831	0.1600	
5	40	1.6526	0.3564	1.6500	-0.0898	2.5146	0.8536	0.1600	P
5	41	1.6374	0.4085	0.7493	0.5920	1.6810	0.8458	0.1500	
5	42	1.6541	0.4137	1.2456	0.1940	1.4692	0.8544	0.1600	
5	43	1.6105	0.3991	1.1854	0.2038	1.9506	0.8319	0.1500	
5	44	1.7025	0.7739	0.5063	0.4932	3.5935	0.8794	0.1400	
5	45	1.7025	0.7739	0.6884	0.3366	3.5935	0.8794	0.1400	
5	46	1.6920	0.4082	1.2721	0.2152	1.3719	0.8739	0.1600	
5	47	1.6760	0.3278	1.0429	0.4408	1.8692	0.8657	0.1300	

LIST OF REFERENCES

Dixon, W. J., 1970: Biomedical Computer Programs. University of California Publication in Auto. Comp., No. 2.

Downey, P. H., Lassman, S. J. and Vonder Haar, T. H., 1972: A study of extreme and persistent cloudiness based on satellite observations (1969-1970), Colorado State University Tech. Report.

Fritz, S., Krishna Rao, P., and Weinstein, M., 1964: Satellite measurements of reflected solar energy and the energy received at the ground. Journal Atmos. Sci., 21, pp. 141-151.

Gabites, J. F., 1950: Seasonal variations in the atmospheric heat balance. ScD. thesis, Massachusetts Institute of Technology.

Hanson, K. J., 1971: Studies of cloud and satellite parameterization of solar irradiance at the earth's surface. Proceedings of the Miami Workshop on Remote Sensing, U. S. Department of Commerce.

Hanson, K. J., Hickey, J. and Scholes, W., 1972: A report on the pyranometer calibration program of the U. S. Weather Bureau, ESSA and NOAA 1954-1972. In publication.

Hanson, K. J., Vonder Haar, T. H. and Suomi, V. E., 1967: Reflection of sunlight to space and absorption by the earth and atmosphere over the U. S. during Spring 1962. Mon. Wea. Rev., 95, 6, pp. 354-362.

Houghton, H. G., "On the Annual Heat Balance of the Northern Hemisphere," Journal of Meteorology, Vol. 11, No. 1, Feb. 1954, pp. 1-9.

Kung, E. C., Bryson, R. A., and Lenschow, D. H., 1964: Study of a continental surface albedo on the basis of flight measurements and structure of the earth's surface cover over North America. Mon. Wea. Rev., 92, 12, pp. 543-563.

List, R. J. (ed), 1958: Smithsonian Meteorological Tables, Smithsonian Institution, Sixth Edition, Revised.

London, J., 1957: A study of the atmospheric heat balance. Final Report, Contract AF 19(122)-165, College of Engineering, New York University.

Nimbus II Users' Guide, ARACON Geophysics Company; Concord, Massachusetts, July 1966.

Raschke, E., Vonder Haar, T. H., Bandeen, W. R. and Pasternak, M., 1973: The radiation balance of the earth-atmosphere system from Nimbus 3 radiation measurements.

Sellers, W. D., 1965: Physical Climatology. University of Chicago Press.

Vonder Haar, T. H., 1968: Variations of the Earth's Radiation Budget. Meteorological Satellite Instrumentation and Data Processing, Final Scientific Report on NASw-65 1958-1968, University of Wisconsin, pp.31-107.

Yamamoto, Giichi, 1962: Direct Absorption of Solar Radiation by Atmospheric Water Vapor, Carbon Dioxide and Molecular Oxygen. Jour. Atmos. Sci., 19, 2, pp. 182-188.

INITIAL DISTRIBUTION LIST

		No. Copies
1.	Defense Documentation Center Cameron Station Alexandria, Virginia 22314	2
2.	Library, Code 0212 Naval Postgraduate School Monterey, California 93940	2
3.	Professor F. L. Martin, Code 51Mr Department of Meteorology Naval Postgraduate School Monterey, California 93940	7
4.	Lieutenant Donald J. Healy, USN 1224 Calle Santiago Chula Vista, Ca. 92011	5
5.	Department of Meteorology, Code 51 Naval Postgraduate School Monterey, California 93940	1
6.	Naval Weather Service Command Naval Weather Service Headquarters Washington Naval Yard Washington, D. C. 20390	1
7.	Commanding Officer Fleet Numerical Weather Central Monterey, California 93940	1
8.	Commanding Officer Environmental Prediction Research Facility Monterey, California 93940	2

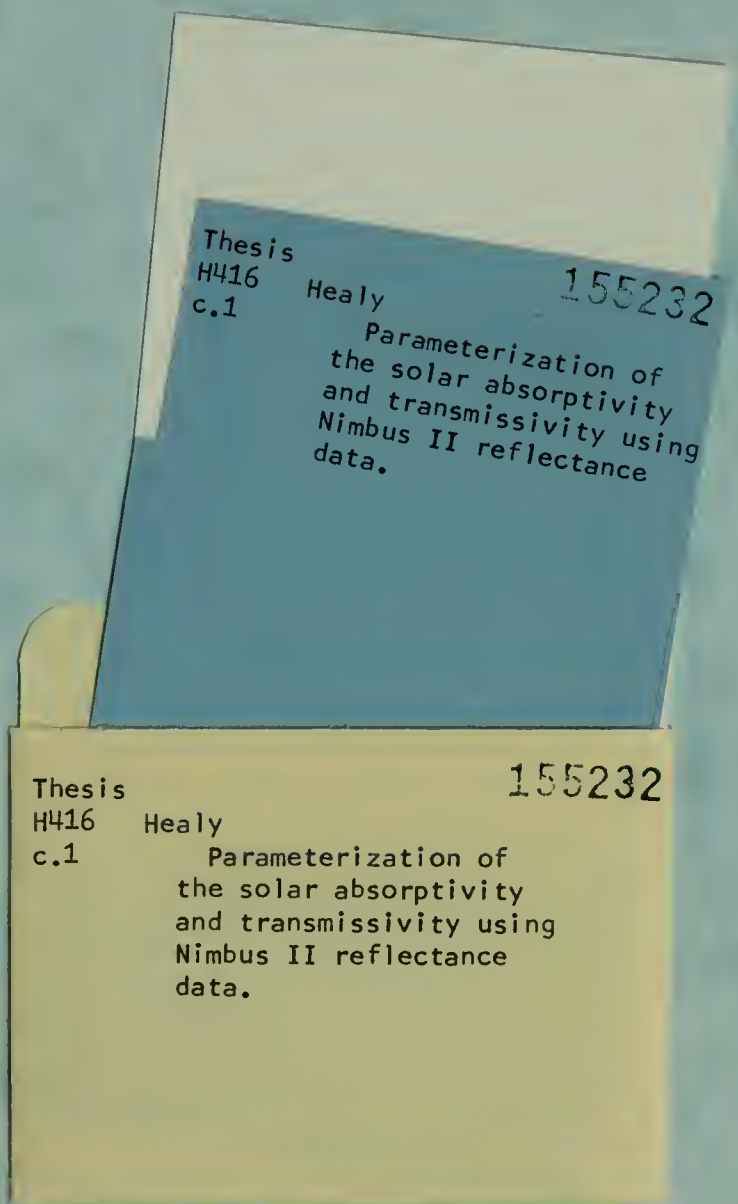

Thesis
H416
c.1
Healy
155232
Parameterization of the solar absorptivity and transmissivity using Nimbus II reflectance data.